

World Journal of *Stem Cells*

World J Stem Cells 2022 July 26; 14(7): 435-576



REVIEW

- 435 Therapeutic potential of dental pulp stem cells and their derivatives: Insights from basic research toward clinical applications
Yuan SM, Yang XT, Zhang SY, Tian WD, Yang B
- 453 Role of hypoxia preconditioning in therapeutic potential of mesenchymal stem-cell-derived extracellular vesicles
Pulido-Escribano V, Torrecillas-Baena B, Camacho-Cardenosa M, Dorado G, Gálvez-Moreno MÁ, Casado-Díaz A
- 473 Application of exosome-derived noncoding RNAs in bone regeneration: Opportunities and challenges
Ren YZ, Ding SS, Jiang YP, Wen H, Li T
- 490 Metabolic-epigenetic nexus in regulation of stem cell fate
Liu Y, Cui DX, Pan Y, Yu SH, Zheng LW, Wan M

MINIREVIEWS

- 503 Stem cell therapy for insulin-dependent diabetes: Are we still on the road?
Yang L, Hu ZM, Jiang FX, Wang W
- 513 Prodigious therapeutic effects of combining mesenchymal stem cells with magnetic nanoparticles
Abu-El-Rub E, Khasawneh RR, Almahasneh F

ORIGINAL ARTICLE**Basic Study**

- 527 Application of extracellular vesicles from mesenchymal stem cells promotes hair growth by regulating human dermal cells and follicles
Rajendran RL, Gangadaran P, Kwack MH, Oh JM, Hong CM, Sung YK, Lee J, Ahn BC
- 539 miR-3682-3p directly targets FOXO3 and stimulates tumor stemness in hepatocellular carcinoma *via* a positive feedback loop involving FOXO3/PI3K/AKT/c-Myc
Chen Q, Yang SB, Zhang YW, Han SY, Jia L, Li B, Zhang Y, Zuo S
- 556 Intratracheal administration of umbilical cord-derived mesenchymal stem cells attenuates hyperoxia-induced multi-organ injury *via* heme oxygenase-1 and JAK/STAT pathways
Dong N, Zhou PP, Li D, Zhu HS, Liu LH, Ma HX, Shi Q, Ju XL

ABOUT COVER

Editorial Board Member of *World Journal of Stem Cells*, Wei Zhang, PhD, Associated Professor, School of Medicine, Southeast University, No. 87 Ding Jiaqiao, Nanjing 210009, Jiangsu Province, China. zhang.wei@seu.edu.cn

AIMS AND SCOPE

The primary aim of *World Journal of Stem Cells (WJSC, World J Stem Cells)* is to provide scholars and readers from various fields of stem cells with a platform to publish high-quality basic and clinical research articles and communicate their research findings online. *WJSC* publishes articles reporting research results obtained in the field of stem cell biology and regenerative medicine, related to the wide range of stem cells including embryonic stem cells, germline stem cells, tissue-specific stem cells, adult stem cells, mesenchymal stromal cells, induced pluripotent stem cells, embryonal carcinoma stem cells, hemangioblasts, lymphoid progenitor cells, *etc.*

INDEXING/ABSTRACTING

The *WJSC* is now abstracted and indexed in Science Citation Index Expanded (SCIE, also known as SciSearch®), Journal Citation Reports/Science Edition, PubMed, PubMed Central, Scopus, Biological Abstracts, BIOSIS Previews, Reference Citation Analysis, China National Knowledge Infrastructure, China Science and Technology Journal Database, and Superstar Journals Database. The 2022 Edition of Journal Citation Reports cites the 2021 impact factor (IF) for *WJSC* as 5.247; IF without journal self cites: 5.028; 5-year IF: 4.964; Journal Citation Indicator: 0.56; Ranking: 12 among 29 journals in cell and tissue engineering; Quartile category: Q2; Ranking: 86 among 194 journals in cell biology; and Quartile category: Q2. The *WJSC*'s CiteScore for 2021 is 5.1 and Scopus CiteScore rank 2021: Histology is 17/61; Genetics is 145/335; Genetics (clinical) is 42/86; Molecular Biology is 221/386; Cell Biology is 164/274.

RESPONSIBLE EDITORS FOR THIS ISSUE

Production Editor: Yan-Liang Zhang; Production Department Director: Xu Guo; Editorial Office Director: Jia-Ru Fan.

NAME OF JOURNAL

World Journal of Stem Cells

ISSN

ISSN 1948-0210 (online)

LAUNCH DATE

December 31, 2009

FREQUENCY

Monthly

EDITORS-IN-CHIEF

Shengwen Calvin Li, Carlo Ventura

EDITORIAL BOARD MEMBERS

<https://www.wjgnet.com/1948-0210/editorialboard.htm>

PUBLICATION DATE

July 26, 2022

COPYRIGHT

© 2022 Baishideng Publishing Group Inc

INSTRUCTIONS TO AUTHORS

<https://www.wjgnet.com/bpg/gerinfo/204>

GUIDELINES FOR ETHICS DOCUMENTS

<https://www.wjgnet.com/bpg/GerInfo/287>

GUIDELINES FOR NON-NATIVE SPEAKERS OF ENGLISH

<https://www.wjgnet.com/bpg/gerinfo/240>

PUBLICATION ETHICS

<https://www.wjgnet.com/bpg/GerInfo/288>

PUBLICATION MISCONDUCT

<https://www.wjgnet.com/bpg/gerinfo/208>

ARTICLE PROCESSING CHARGE

<https://www.wjgnet.com/bpg/gerinfo/242>

STEPS FOR SUBMITTING MANUSCRIPTS

<https://www.wjgnet.com/bpg/GerInfo/239>

ONLINE SUBMISSION

<https://www.f6publishing.com>

Basic Study

Intratracheal administration of umbilical cord-derived mesenchymal stem cells attenuates hyperoxia-induced multi-organ injury via heme oxygenase-1 and JAK/STAT pathways

Na Dong, Pan-Pan Zhou, Dong Li, Hua-Su Zhu, Ling-Hong Liu, Hui-Xian Ma, Qing Shi, Xiu-Li Ju

Specialty type: Cell and tissue engineering**Provenance and peer review:** Unsolicited article; Externally peer reviewed.**Peer-review model:** Single blind**Peer-review report's scientific quality classification**Grade A (Excellent): 0
Grade B (Very good): B
Grade C (Good): C
Grade D (Fair): 0
Grade E (Poor): 0**P-Reviewer:** Kanamoto T, Japan; Zhang Q, China**Received:** March 30, 2022**Peer-review started:** March 30, 2022**First decision:** April 25, 2022**Revised:** May 4, 2022**Accepted:** June 20, 2022**Article in press:** June 20, 2022**Published online:** July 26, 2022**Na Dong, Hua-Su Zhu,** Department of Pediatrics, Qilu Hospital, Cheeloo College of Medicine, Shandong University, Jinan 250012, Shandong Province, China**Pan-Pan Zhou, Xiu-Li Ju,** Department of Pediatrics, Qilu Hospital of Shandong University, Jinan 250012, Shandong Province, China**Dong Li, Ling-Hong Liu, Hui-Xian Ma, Qing Shi, Xiu-Li Ju,** Stem Cell and Regenerative Medicine Research Center, Qilu Hospital of Shandong University, Jinan 250012, Shandong Province, China**Corresponding author:** Xiu-Li Ju, PhD, Chief Doctor, Department of Pediatrics, Qilu Hospital of Shandong University, No. 107 Wenhua West Road, Jinan 250012, Shandong Province, China. jxlqlyy@163.com

Abstract

BACKGROUND

Bronchopulmonary dysplasia (BPD) is not merely a chronic lung disease, but a systemic condition with multiple organs implications predominantly associated with hyperoxia exposure. Despite advances in current management strategies, limited progress has been made in reducing the BPD-related systemic damage. Meanwhile, although the protective effects of human umbilical cord-derived mesenchymal stem cells (hUC-MSCs) or their exosomes on hyperoxia-induced lung injury have been explored by many researchers, the underlying mechanism has not been addressed in detail, and few studies have focused on the therapeutic effect on systemic multiple organ injury.

AIM

To investigate whether hUC-MSC intratracheal administration could attenuate hyperoxia-induced lung, heart, and kidney injuries and the underlying regulatory mechanisms.

METHODS

Neonatal rats were exposed to hyperoxia (80% O₂), treated with hUC-MSCs intratracheal (iT) or intraperitoneal (iP) on postnatal day 7, and harvested on postnatal day 21. The tissue sections of the lung, heart, and kidney were analyzed morphometrically. Protein contents of the bronchoalveolar lavage fluid (BALF), myeloper-

oxidase (MPO) expression, and malondialdehyde (MDA) levels were examined. Pulmonary inflammatory cytokines were measured *via* enzyme-linked immunosorbent assay. A comparative transcriptomic analysis of differentially expressed genes (DEGs) in lung tissue was conducted *via* RNA-sequencing. Subsequently, we performed reverse transcription-quantitative polymerase chain reaction and western blot analysis to explore the expression of target mRNA and proteins related to inflammatory and oxidative responses.

RESULTS

iT hUC-MSCs administration improved pulmonary alveolarization and angiogenesis ($P < 0.01$, $P < 0.01$, $P < 0.001$, and $P < 0.05$ for mean linear intercept, septal counts, vascular medial thickness index, and microvessel density respectively). Meanwhile, treatment with hUC-MSCs iT ameliorated right ventricular hypertrophy (for Fulton's index, $P < 0.01$), and relieved reduced nephrogenic zone width ($P < 0.01$) and glomerular diameter ($P < 0.001$) in kidneys. Among the beneficial effects, a reduction of BALF protein, MPO, and MDA was observed in hUC-MSCs groups ($P < 0.01$, $P < 0.001$, and $P < 0.05$ respectively). Increased pro-inflammatory cytokines tumor necrosis factor- α , interleukin (IL)-1 β , and IL-6 expression observed in the hyperoxia group were significantly attenuated by hUC-MSCs administration ($P < 0.01$, $P < 0.001$, and $P < 0.05$ respectively). In addition, we observed an increase in anti-inflammatory cytokine IL-10 expression in rats that received hUC-MSCs iT compared with rats reared in hyperoxia ($P < 0.05$). Transcriptomic analysis showed that the DEGs in lung tissues induced by hyperoxia were enriched in pathways related to inflammatory responses, epithelial cell proliferation, and vasculature development. hUC-MSCs administration blunted these hyperoxia-induced dysregulated genes and resulted in a shift in the gene expression pattern toward the normoxia group. hUC-MSCs increased heme oxygenase-1 (HO-1), JAK2, and STAT3 expression, and their phosphorylation in the lung, heart, and kidney ($P < 0.05$). Remarkably, no significant difference was observed between the iT and iP administration.

CONCLUSION

iT hUC-MSCs administration ameliorates hyperoxia-induced lung, heart, and kidney injuries by activating HO-1 expression and JAK/STAT signaling. The therapeutic benefits of local iT and iP administration are equivalent.

Key Words: Mesenchymal stem cell; Hyperoxia; Multiple organ injury; Bronchopulmonary dysplasia; Heme oxygenase-1; JAK/STAT pathway

©The Author(s) 2022. Published by Baishideng Publishing Group Inc. All rights reserved.

Core Tip: In the present study, we used a newborn rat model of postnatal hyperoxia exposure to simulate clinical bronchopulmonary dysplasia (BPD) and the associated heart and kidney injuries in preterm infants. Improved lung, heart, and kidney development, as well as reduced inflammatory and oxidative responses, were observed with human umbilical cord-derived mesenchymal stem cells (hUC-MSCs) administration. We demonstrated that hUC-MSCs ameliorate hyperoxia-induced systemic organ injuries by activating heme oxygenase-1 expression and JAK/STAT pathway. Overall, our study shows that intratracheal administration is a more attractive route of MSCs administration in preterm infants for the prevention and treatment of BPD and hyperoxia-induced systemic damage.

Citation: Dong N, Zhou PP, Li D, Zhu HS, Liu LH, Ma HX, Shi Q, Ju XL. Intratracheal administration of umbilical cord-derived mesenchymal stem cells attenuates hyperoxia-induced multi-organ injury *via* heme oxygenase-1 and JAK/STAT pathways. *World J Stem Cells* 2022; 14(7): 556-576

URL: <https://www.wjgnet.com/1948-0210/full/v14/i7/556.htm>

DOI: <https://dx.doi.org/10.4252/wjsc.v14.i7.556>

INTRODUCTION

Bronchopulmonary dysplasia (BPD) is the most common chronic lung disease in premature infants and is a heterogeneous disease predominantly associated with oxygen supplementation clinically[1]. Data from major cohort studies demonstrate an increasing BPD prevalence of 11%-50%, most likely due to the increased survival of newborns at an extremely low gestational age[2,3]. Current management strategies include the use of volume-targeted and non-invasive ventilation, as well as targeted use of

steroids along with adjunct medical therapies including surfactant, caffeine, and vitamin A[2,4]. Despite advances in these interventions resulting in improved survival and decreased morbidity, limited progress has been made in reducing the risk of BPD development.

BPD is characterized by varying magnitudes of impairment in alveolar septation, lung fibrosis, and abnormal vascular development and remodeling. Moreover, increasing evidence has suggested that BPD is not merely a lung disease but a systemic condition with short-term and long-term multiple organ implications[3,5]. Clinical and experimental findings demonstrated that chronic exposure to hyperoxia causes oxidative stress and leads to certain implications, including neurodevelopmental impairments [6], retinopathy of prematurity[7,8], renal vascular and tubular development impairments[9,10], and associated cardiac disease[11,12]. Notably, hyperoxia exposure in neonates results in long-term cardiac defects and renal abnormalities in later adult life. More specifically, recent studies on experimental models have revealed that hyperoxia-treated mice exhibited significantly reduced stroke volume and ejection fractions, the appearance of left ventricular (LV) dysfunction, right ventricular (RV) dysfunction, and pulmonary hypertension (PH)[13,14]. In addition, hyperoxia exposure reduces kidney size, glomerular density, and glomerular filtration rate, along with increases in the renal tubular necrosis, dilation, regeneration, and interstitial inflammation[10,15]. Hence, new effective therapeutic interventions are urgently needed to attenuate BPD-associated multiple organ damage, rather than focusing on single organ injuries.

Mesenchymal stem cells (MSCs) are multipotent stromal cells that have immunomodulatory and anti-inflammatory properties, as well as low immunogenicity, and have shown great potential for the management of a range of different neonatal conditions, including BPD, in both preclinical models and clinical trials, by systemic or local intratracheal (iT) administration[16-20]. The therapeutic mechanism of MSCs may predominantly include paracrine or indirect pathways, which are responsible for the beneficial effects of local MSCs administration on systemic damage[21,22]. Neonates with very low birth weight are often intubated at birth, making local iT instillation an attractive route of administration[17]. Notably, higher isolation efficiency and proliferation capacity, lower immunogenicity, and greater overall immunomodulatory and anti-inflammatory effects were observed for human umbilical cord-derived MSCs (hUC-MSCs) over stem cells harvested from other sources[23]. Moreover, recent studies confirmed that MSCs are poorly immunogenic, and both allogeneic and xenogeneic MSCs showed equal efficacy without side effects[24,25]. Xenogeneic hUC-MSCs transplantation has been extensively investigated over the past decades on various animal models with promising effects[16,18,19]. However, beyond the pulmo-protective properties of systemic or local iT hUC-MSCs administration, its potential therapeutic effects on hyperoxia-induced heart and kidney injuries have not yet been evaluated.

Extensive evidence has demonstrated that heme oxygenase-1 (HO-1) is an inducible enzyme with potent anti-oxidant, anti-inflammatory, and anti-apoptotic attributes[26,27]. The protective response regulated by HO-1 has been reported in multiple animal models of hyperoxia-induced injury[28-30]. Furthermore, it is generally considered that the JAK2 and STAT3 signaling pathway are involved in the various patho-physiological responses[31] and also play a key role in the development of pulmonary [32], cardiovascular[33], and renal[34] diseases. Interestingly, the evidence demonstrated that cross-talk may exist between HO-1 and JAK/STAT pathways[35-37]. However, whether HO-1 and JAK/STAT signaling pathways are involved in the protective effects of MSCs remains unclear.

In the present study, we used a newborn rat model of postnatal hyperoxia exposure to simulate clinical BPD and the associated heart and kidney injuries in preterm infants. This study aimed to investigate whether iT administration of hUC-MSCs could simultaneously attenuate hyperoxia-induced lung, heart, and kidney injuries in experimental neonatal rat models *via* mechanisms that involve activation of the HO-1 and JAK2/STAT3 signaling pathways.

MATERIALS AND METHODS

hUC-MSCs culture and identification

hUC-MSCs were provided by the Cell and tissue bank of Shandong province (Jinan, China) and cultured in alpha-minimal essential medium (Gibco, Carlsbad, CA, United States) containing 10% fetal bovine serum and 1% penicillin/streptomycin (Gibco) at 37 °C with 5% CO₂. Cells between passage three and five were used in this study.

Phenotypic analysis was conducted by flow cytometry[38]. Briefly, hUC-MSCs were washed with phosphate-buffered saline (PBS) and resuspended to a concentration of 1×10^6 cells/mL. Then, the cells were stained with antibodies against the following cell surface epitopes: Phycoerythrin (PE)-anti CD29 (1:20; 303004, BioLegend, San Diego, CA, United States), PE-anti CD31 (303106, BioLegend), PE-anti CD44 (12-0441-82, eBioscience, San Diego, CA, United States), PE-anti CD45 (368510, BioLegend), PE-anti CD73 (344004, BioLegend), PE-anti CD90 (12-0909-42, eBioscience), PE-anti CD105 (12-1057-42, eBioscience), and PE-anti CD271 (12-9400-42, eBioscience). Flow cytometry was performed with the Guava easyCyte 6HT (EMD Millipore, Billerica, MA, United States), and the data were examined using the Flowjo™ software (V10, BD Life Sciences, Franklin Lakes, NJ, United States). To demonstrate the multilineage differentiation potential, hUC-MSCs were seeded in 6-well plates and cultured in

adipogenic (HUXUC-90031, Cyagen, Santa Clara, CA, United States), and osteogenic (HUXUC-90021, Cyagen) differentiation medium, or in a loosely capped tube (430790, Corning, NY, United States) in chondrogenic differentiation (HUXUC-90042, Cyagen) medium. The medium was changed every 3 d in accordance with the manufacturer's instructions. At the end of 21 d, all cells were fixed with 4% paraformaldehyde (PFA) and processed with oil red O, alizarin red, and alcian blue.

Animal model and experimental groups

Timed pregnant Sprague Dawley rats were obtained from SPF (Beijing) Biotechnology Co., Ltd. (Beijing, China) and kept under a 12/12 h light-dark cycle, controlled temperature of 25 ± 2 °C, and relative humidity of 55% ($\pm 10\%$) with free access to food and water. Pregnant rats were housed individually and allowed to deliver vaginally at term. Newborn rats were then randomly assigned to four experimental groups as follows: Normoxia group ($n = 12$, exposed to room air), hyperoxia group [$n = 12$, exposed to 80% O₂, treated with PBS 40 μ L on postnatal day 7 (P7)], hyperoxia + iT-MSC group ($n = 12$, exposed to 80% O₂, treated with 4×10^5 hUC-MSCs, 40 μ L, iT, on P7), and hyperoxia + intraperitoneal (iP)-MSC group ($n = 12$, exposed to 80% O₂, treated with 4×10^5 hUC-MSCs, 40 μ L, iP, on P7). The nursing mothers were alternated between the 80% O₂ and the room air groups every 24 h to minimize oxygen toxicity in the mothers.

On postnatal day 21 (P21), rats were euthanized *via* iP injection of pentobarbital sodium. Bronchoalveolar lavage fluid (BALF) was obtained after ligation of the right main bronchus by back-flushing 1 mL of cold PBS three times *via* endotracheal intubation. The lungs, heart, and kidneys were excised and fixed overnight in 4% PFA for histological analysis, or frozen at -80 °C for reverse transcription-quantitative polymerase chain reaction (RT-qPCR), western blotting, and cytokine analyses. All animal procedures and protocols complied with the National Institutes of Health Guide for the Care and Use of Laboratory Animals and were approved by the Ethics Committee on Animal Experiments of Shandong University Qilu Hospital (DWLL-2021-035, Jinan, China).

iT administration

For iT administration, the neonatal rats on P7 were euthanized *via* iP injection of pentobarbital sodium and restrained on a board with the neck in hyperflexion. The 29-gauge needle syringe (320310, Becton, Dickinson and Company, NJ, United States) with the tip smoothed and wrapped with a 0.3 mm flexible capillary pipe was prepared as endotracheal intubation. The light source was placed close to the neck of the rat. The rat's tongue was wrapped and pulled outside the mouth with gauze in the right hand, the root of the tongue was gently pressed with a small tweezer to expose the glottis with the left hand. hUC-MSCs were transplanted into the trachea through the prepared endotracheal intubation at the glottis opening. Then the rats were allowed to recover from the anesthesia and return to their dam. Mortality induced by the iT administration procedure was not observed.

Protein content in BALF

BALF was centrifuged at 3000 rpm for 20 min at 4 °C, and the supernatant was collected into a new tube. The protein content of cell-free BALF was subsequently measured using the BCA Protein Quantitative Assay Kit (Beyotime Biotechnology, Shanghai, China) in accordance with the manufacturer's instructions and was used as an indication of endothelial and epithelial permeability.

Histological examination

The lung, heart, and kidney tissues were fixed in 4% PFA, washed with PBS, and then serially dehydrated in increasing concentrations of ethanol before being embedded in paraffin. Consecutive sections (5 μ m thick) from each tissue block were subjected to hematoxylin and eosin (HE) staining, observed under a microscope (Olympus, BH2, Japan), and photographed (CellSens, Ver. 1.18, Japan). Alveolar structures in lung sections were quantified using the mean linear intercept (MLI) and septal count methods[17,39]. Briefly, the number of intercepts was counted in both the horizontal and vertical fields, and MLI was measured following the equation $MLI = N \times L/m$, where m is the sum of all the intercepts, L is the length of the traverses, and N is the number of times the traverses were placed on the lung. To quantify the degree of PH-induced right ventricular hypertrophy (RVH), the thicknesses of the right ventricle (RV) free wall, left ventricle (LV) free wall, and interventricular septum (IVS) of excised hearts were measured, and $RV/LV + IVS$ (Fulton's index) was calculated[12,21]. The kidney sections across the full coronal plane were stained for morphology assessment as previously described by Mohr *et al*[15]. Glomerular diameter and width of the nephrogenic zone were measured. Five measurements of each parameter in each of the three fields of view were recorded and then averaged. All the above parameters were measured using Image Pro Plus (V6.0, Media Cybernetics, United States).

Immunohistochemistry and immunofluorescence

Immunohistochemistry (IHC) and immunofluorescence (IF) were performed on 5 μ m paraffin sections. After routine deparaffinization, heat-induced epitope retrieval was performed by immersing the slides in 0.01 M sodium citrate buffer (pH = 6.0). The sections were preincubated in 0.3% hydrogen peroxide for 10 min to remove the endogenous peroxidase activity and then in 0.1 M PBS containing 5% normal

goat serum for 1 h at room temperature to block the non-specific antibody binding. Subsequently, the samples were stained with rabbit anti- α smooth muscle actin (α -SMA) antibody (1:100; 19245S, CST, Danvers, MA, United States), or rabbit anti-von Willebrand factor (vWF) polyclonal antibody (1:50; 27186-1-AP, Proteintech, Rosemont, IL, United States) as primary antibodies overnight at 4 °C. For IHC, sections were then incubated with horseradish peroxidase (HRP)-labeled goat anti-rabbit/mouse IgG polymers (PK10006, Proteintech), developed in 3,3'-diaminobenzidine (Proteintech) and counterstained with hematoxylin following the manufacturer's recommendations. For IF, the samples were incubated with DyLight® 488 pre-adsorbed secondary antibodies (ab98498, Abcam, Cambridge, United Kingdom) for 1 h at 37 °C and cell nuclei were counterstained with DAPI for 15 min. The thickness of the microvessel muscle layers was measured using sections stained with anti- α -SMA and the medial thickness index (MTI) was calculated as follows: $(A_{ext} - A_{int})/A_{ext}$, where A_{ext} and A_{int} are the areas within the external and internal boundaries of the α -SMA layer, respectively[17]. Pulmonary microvessel density (MVD) was determined by counting the number of vWF-positive vessels ($< 100 \mu\text{m}$) per high-power field using Image J (V1.8, National Institutes of Health, United States)[16].

Malondialdehyde concentration in tissues

Frozen lung, heart, and kidney tissues were weighed, and 10% tissue homogenate was prepared at 4 °C using an electric tissue grinder (LC-TG-24, Lichen Keyi, Shanghai, China). Malondialdehyde (MDA) levels in the tissues were measured using colorimetric assay kits in accordance with the manufacturer's instructions (BC0025, Solarbio, Beijing, China). The absorbance of the organic layer was measured using spectrophotometry at 450, 532, and 600 nm (DNM-9602, Perlong, Beijing, China). MDA levels were expressed in mmol/g wet tissue and calculated as follows: $[12.9 \times (\Delta A_{532} - \Delta A_{600}) - 2.58 \times \Delta A_{450}] \times 50$.

Myeloperoxidase level in tissues

The tissues were homogenized to determine the expression of myeloperoxidase (MPO) in accordance with the manufacturer's instructions (A044-1-1, Jchio, Nanjing, China). Yellow compounds were produced on hydrogen supply from adjacent anisodamines, and the amount was measured at 460 nm to reflect the viability of MPO and the number of leukocytes. One unit of MPO activity was defined as the quantity of enzyme that degrades 1 μmol peroxide/min.

Quantitation of cytokine levels by enzyme-linked immunosorbent assay

The total protein content of lung tissue homogenate was measured and samples were analyzed using the rat interleukin (IL)-1 β (KE20005, Proteintech), IL-10 (KE20003, Proteintech), tumor necrosis factor- α (TNF- α) (KE20001, Proteintech), and IL-6 (SEKR-0005, Solarbio, China) enzyme-linked immunosorbent assay (ELISA) kits to determine the level of inflammatory cytokines in accordance with the manufacturer's instructions. The absorbance was measured at 450 nm.

RNA extraction and RT-qPCR

Total RNA was extracted from the lung samples using TRIzol reagent (T9424-100 mL, Sigma, United States) according to the manufacturer's protocols. First-strand cDNA was synthesized from 1 μg of total RNA using the ReverTraAce RT-qPCR Master Mix kit (FSQ-201, TOYOBO, Osaka, Japan). RT-qPCR was performed using a Real-Time Thermocycler (Analytik Jena AG, qTOWER3G, Germany), and detection was performed using SYBR Green Realtime PCR Master Mix (TOYOBO, Osaka, Japan) in a 20 μL reaction mixture to detect the mRNA levels of relative genes. All procedures were performed according to the manufacturer's protocol. The primer sequences for each gene analyzed using RT-qPCR are listed in Table 1. The cycling profile involved 40 cycles of the following: 95 °C for 5 s, 55 °C for 10 s, and 72 °C for 15 s. Data were analyzed using Sequence Detection Software 1.4 (Applied Biosystems, CA, United States). Relative fold changes were normalized to endogenous β -actin mRNA expression using the $2^{-\Delta\Delta C_t}$ method.

RNA-sequencing and analysis

The right lower lobe of the lung from the normoxia, hyperoxia, and hyperoxia + iT-MSC groups were collected for total RNA extraction, as mentioned above. Poly-A pull-down with Oligo(dT) was then used to enrich mRNAs from total RNA samples. Then, cDNA libraries were constructed *via* PCR amplification and sequenced using Illumina HiSeq X10 platform (Annoroad Genomics, Beijing, China). Adapter polluted reads and low-quality reads in the original sequence were filtered, and the obtained high-quality clean reads were mapped to the human reference genome (GRCh38) using hierarchical indexing for spliced alignment of transcripts 2 (HISAT2; version 2.2.1). Gene expression levels were measured according to the fragments *per kilobase per million* mapped fragments method. Differentially expressed genes (DEGs) were screened using DESeq2, with absolute \log_2 fold change ≥ 1 and adjusted $P < 0.05$ as criteria. Gene Ontology (GO) enrichment analyses were performed to find significantly enriched GO terms related to the DEGs.

Table 1 Primer sequences for quantitative reverse transcription-polymerase chain reaction

Genes		Sequence (5'- 3')	Length (bp)
MIP-1 α	F	GCTTCTCCTATGGACGGCAA	20
	R	TGCCGGTTTCTCTGGTCAG	20
MIP-1 β	F	CTGCTTCTTACACCTCCCG	21
	R	AAAGGCTGCTGGTCTCATAGT	21
VEGF	F	GCGGATCAAACCTCACCAAAG	21
	R	TGGTCTGCATTCACATCTGCT	22
PDGF	F	CTCTGCTGTACCTGCGTCT	20
	R	TGGGTCATGTTCAAGTCCA	20
β -actin	F	CTCTGTGGATTGGTGGCT	20
	R	CGCAGCTCAGTAACAGTCCG	20

MIP: Macrophage inflammatory protein; VEGF: Vascular endothelial-derived growth factor; PDGF: Platelet-derived growth factor; F: Forward primer; R: Reverse primer.

Western blot analysis

Lung tissue samples were lysed in radioimmunoprecipitation assay buffer (P0013B, Beyotime) containing a phosphatase inhibitor and protease inhibitor mixture. The samples were centrifuged at 12000 rpm for 20 min at 4 °C to remove the cellular debris. Protein concentrations were determined using a BCA protein assay kit (Beyotime). Equal quantities of proteins were separated *via* sodium dodecyl sulfate-polyacrylamide gel electrophoresis and transferred onto polyvinylidene fluoride membranes (ISEQ00010, Millipore, MA, United States). Membranes were blocked in 5% skimmed milk for 1 h at room temperature and then incubated with the following primary antibodies overnight at 4 °C: Rabbit anti-glyceraldehyde-3-phosphate dehydrogenase (GAPDH) (1:3000; 5174S, CST), rabbit anti-Janus kinase 2 (JAK2; 1:1000; 3230S, CST), rabbit anti-phospho-JAK2 (1:1000; 3776S, CST), rabbit anti-signal transducer and activator of transcription 3 (STAT3; 1:2000; 4904S, CST), rabbit anti-phospho-STAT3 (1:2000; 9145S, CST), and rabbit anti-HO-1 (HO-1; 1:1000, 43966S, CST). Membranes were washed and then incubated with HRP-conjugated goat anti-rabbit antibodies (1:5,000; SA00001-2, Proteintech) for 1 h at room temperature. The protein bands were visualized using the ECL chemiluminescence detection kit (Millipore) and analyzed with JP-K600plus (Jiapeng Technology Co., Shanghai, China). The band intensity was quantified using ImageJ software. The signal intensities of all target proteins were normalized to those of GAPDH. The experiments were performed in triplicate.

Statistical analysis

GraphPad Prism 8.0.1 (GraphPad Software, Inc., La Jolla, CA, United States) and SPSS Statistics 26.0 (SPSS, Inc., Chicago, IL, United States) were used for statistical analysis. The quantitative data were examined by normal distribution test and expressed as the mean \pm standard error, followed by variance homogeneity test. One-way analysis of variance (ANOVA) was conducted to determine statistically significant differences among multiple homogeneous groups. For significant ANOVA results, Bonferroni's multiple comparison test was performed to analyze the differences between two groups. Results with *P* values less than 0.05 were considered significant.

RESULTS

Characterization of hUC-MSCs

Typical MSC-associated surface markers were identified by flow cytometry. The hUC-MSCs showed high expression of CD29, CD44, CD73, CD90, and CD105, and did not express endothelial cell marker (CD31), hematopoietic marker (CD45), and differentiated activated effector cell marker (CD271, Figure 1A). The cells were stained with Oil Red O (Figure 1B), Alizarin red (Figure 1C), and Alcian blue (Figure 1D). These results confirmed that the hUC-MSCs could differentiate into osteoblasts, adipocytes, and chondrocytes *in vitro*.

hUC-MSCs administration increases survival rate and improves lung development

Newborn mice were exposed to 80% O₂ or standard room air from P1 to P21. Treatment groups received a single dose of hUC-MSCs iT or iP on P7 (Figure 2A). The survival curve was recorded from the day of

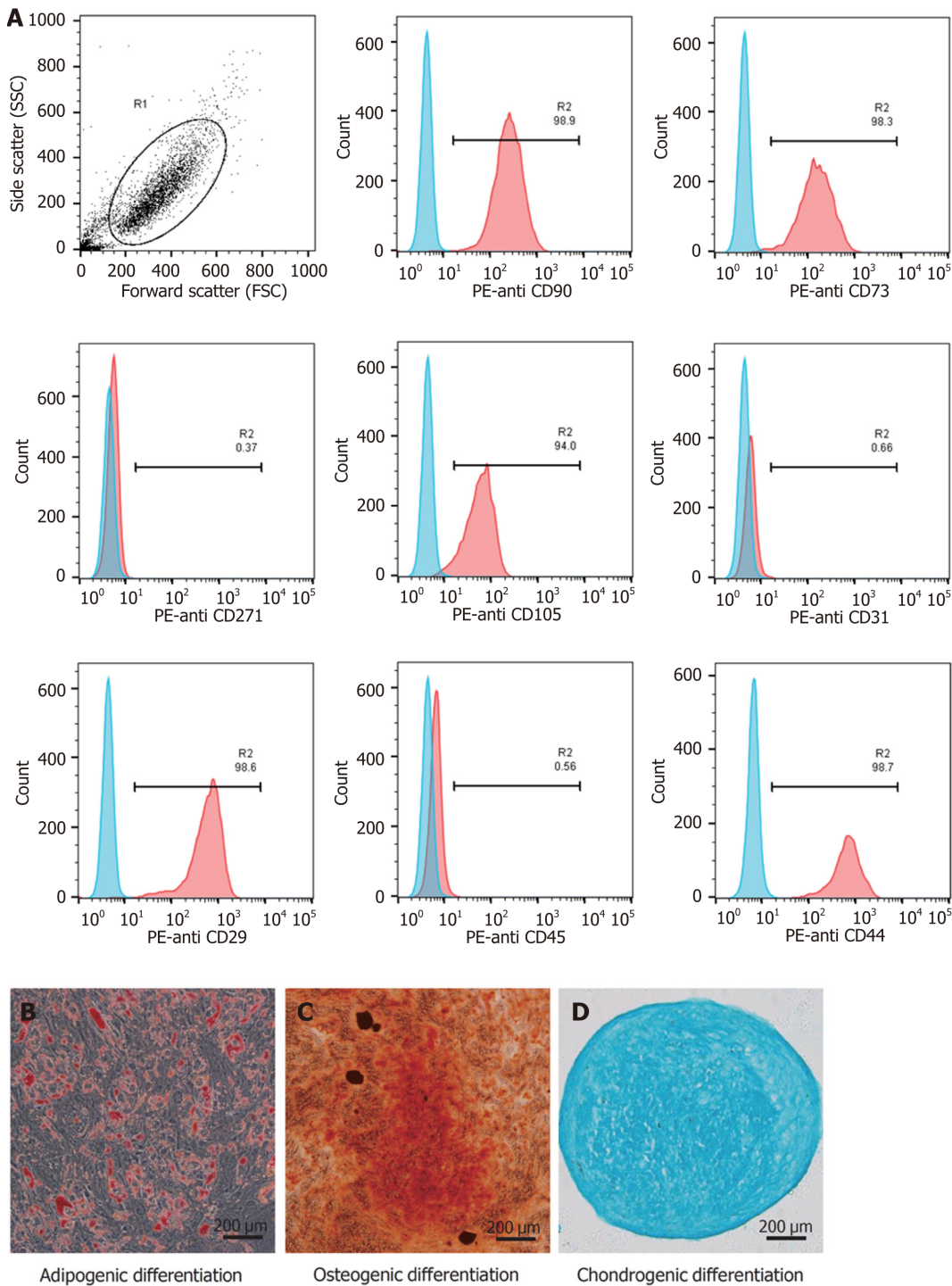
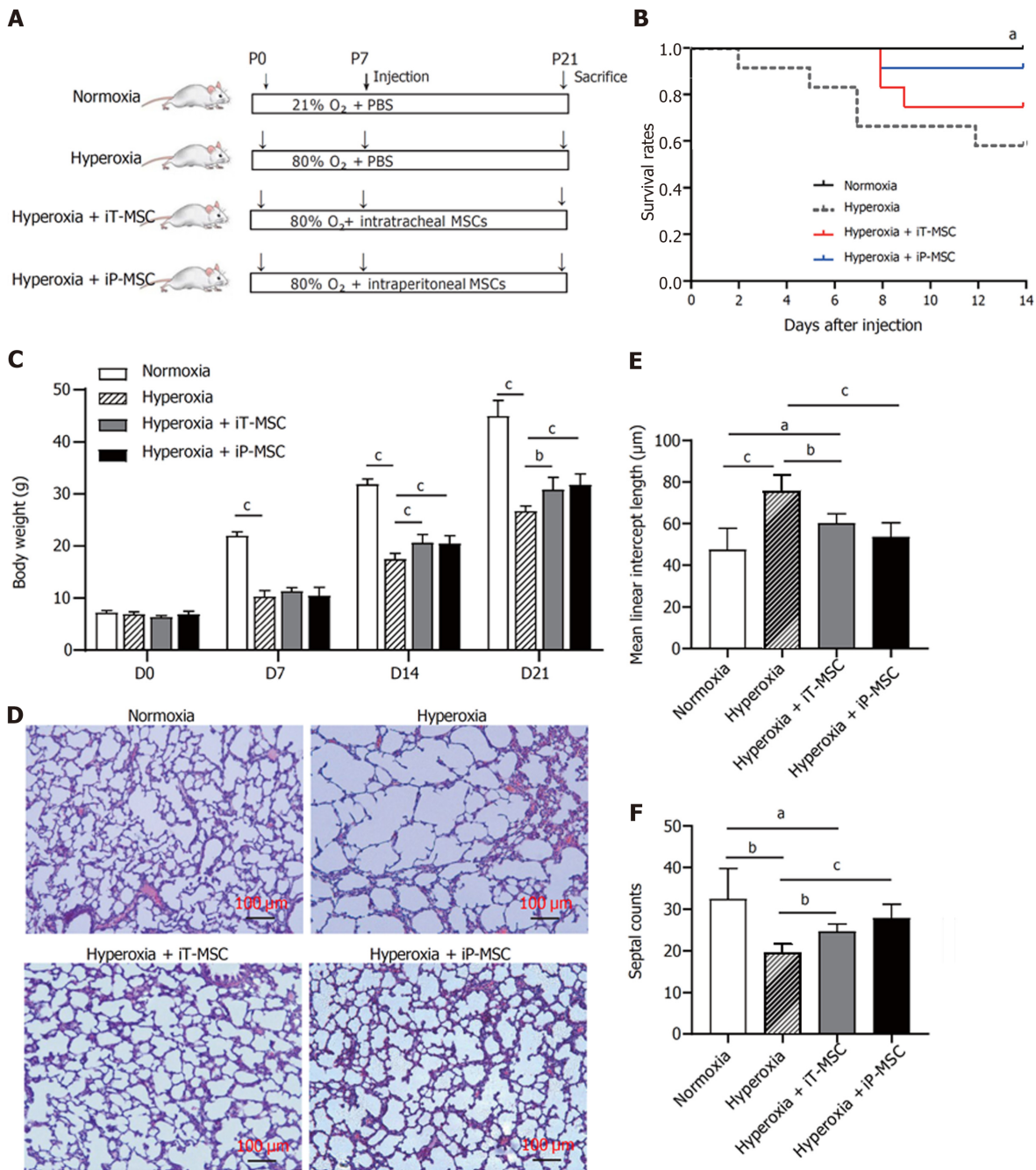


Figure 1 Identification of human umbilical cord-derived mesenchymal stem cells. A: The human umbilical cord-derived mesenchymal stem cells (hUC-MSCs) showed high expression of CD29, CD44, CD73, CD90, and CD105, and did not express CD31, CD45, and CD271; B–D: hUC-MSCs were positive for Oil Red O, Alizarin red, and Alcian blue staining under the corresponding induction conditions (scale bars = 200 μ m).

injection (P7), which was decreased on hyperoxia. iT and iP administration of hUC-MSCs increased the survival of the rats exposed to O_2 , although the difference was not statistically significant (Figure 2B). Remarkably slow growth and body weight gain were observed in rats exposed to hyperoxia from P7, and these were improved on hUC-MSCs administration on P14 and P21 (Figure 2C). There was no statistically significant difference between iT and iP administration.

The lung tissue sections stained with HE showed signs of impaired alveolar development in the animals exposed to hyperoxia, with marked interstitial thickening, fewer septations (hyperoxia *vs* normoxia, 19.55 ± 2.08 *vs* 32.44 ± 7.31 , $P < 0.01$), and enlarged MLI (hyperoxia *vs* normoxia, 76.12 ± 7.7 μ m *vs* 47.34 ± 10.48 μ m, $P < 0.01$; Figure 2D). Treatment with hUC-MSCs significantly diminished the hyperoxia-induced increase in the MLI (60.16 ± 4.62 μ m and 53.65 ± 6.85 μ m for iT-MSC and iP-MSC,



DOI: 10.4252/wjsc.v14.i7.556 Copyright ©The Author(s) 2022.

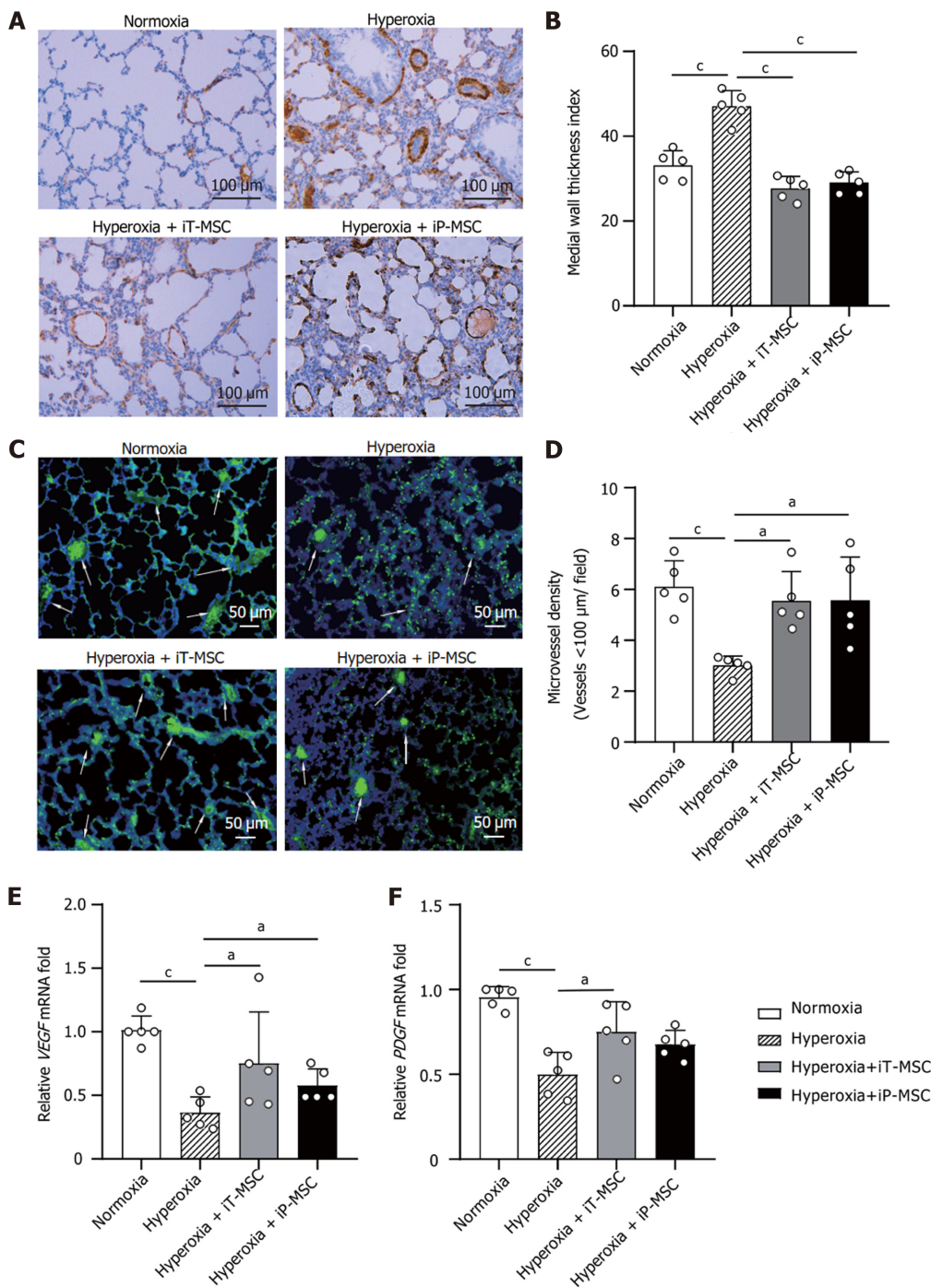
Figure 2 Human umbilical cord-derived mesenchymal stem cells administration increases survival rate and improves lung development.

A: Schematic diagram of the overall experimental design process and grouping; B: Kaplan-Meier survival curves of rat pups treated as indicated; C: Body weight alterations of rat pups treated as indicated; D: Representative images of harvested lung sections stained with hematoxylin and eosin for morphometric analyses (scale bars = 100 μm); E and F: Mean linear intercept and septal counts in lungs treated as indicated (*n* = 5 for each group, 10 fields/animal). ^a*P* < 0.05; ^b*P* < 0.01; ^c*P* < 0.001. iT: Intratracheal; iP: Intraperitoneal; P: Postnatal day; PBS: Phosphate-buffered saline; MSC: Mesenchymal stem cell.

respectively; **Figure 2E**) and decrease in septal counts (24.63 ± 1.85 and 27.84 ± 3.37 for iT-MSC and iP-MSC, respectively; **Figure 2F**).

hUC-MSCs treatment rescues hyperoxia-induced loss of peripheral pulmonary blood vessels and peripheral pulmonary arterial remodeling

To explore the effect of hUC-MSCs on hyperoxia-induced pulmonary vascular remodeling, lung sections were stained with an anti- α -SMA antibody (**Figure 3A**). The MTI for the peripheral pulmonary blood vessels was higher in hyperoxia-exposed animals than that in normoxia-exposed ones (47.18 ± 3.80 vs 33.12 ± 3.48 , *P* < 0.001; **Figure 3B**). The hyperoxia + iT-MSC and hyperoxia + iP-MSC groups exhibited significantly induced vascular muscularization (27.65 ± 2.89 and 29.06 ± 2.52 , respectively).



DOI: 10.4252/wjsc.v14.i7.556 Copyright ©The Author(s) 2022.

Figure 3 Human umbilical cord-derived mesenchymal stem cells treatment rescues hyperoxia-induced loss of peripheral pulmonary blood vessels and peripheral pulmonary arterial remodeling. A: Representative photomicrographs of lung sections of rats harvested at postnatal day 21 stained with α smooth muscle actin antibody in normal air or hyperoxia exposure groups, with or without human umbilical cord-derived mesenchymal stem cells administration (scale bars = 100 μ m); B and D: Medial thickness index and microvessel density in lungs treated as indicated were calculated to assess hyperoxia-induced peripheral pulmonary vascular remodeling and loss of blood vessels in the peripheral microvasculature ($n = 5$ for each group, 5 fields/animal); C: Representative lung slides with von Willebrand factor- immunofluorescence staining obtained at 200 \times magnification. White arrows highlight stained pulmonary vessels (scale bars = 50 μ m); E and F: Vascular endothelial-derived growth factor and platelet-derived growth factor mRNA expression in the lung tissues in the indicated groups. ^a $P < 0.05$; ^b $P < 0.01$; ^c $P < 0.001$. iT: Intratracheal; iP: Intraperitoneal; VEGF: Vascular endothelial-derived growth factor; PDGF: Platelet-derived growth factor; MSC: Mesenchymal stem cell.

To determine the effect of hyperoxia exposure on peripheral pulmonary vessel number, we performed von Willebrand factor staining on lung sections (Figure 3C). The rats reared in hyperoxia yielded a significantly lower MVD than those reared in normoxia (3.01 ± 0.36 vs 6.11 ± 1.02 vessels/field, $P < 0.001$; Figure 3D). Treatment with hUC-MSCs significantly restored the hyperoxia-induced decrease in vascular density (5.54 ± 1.16 and 5.57 ± 1.70 for iT-MSC and iP-MSC, respectively). MTI and MVD of the lungs of the iT-MSC-treated animals did not differ significantly from those of the iP-MSC-treated

group.

Vascular endothelial-derived growth factor (VEGF) and platelet-derived growth factor (PDGF) expression were primarily detected in lung tissues using RT-qPCR. Decreased *VEGF* and *PDGF* mRNA expression was observed in the lungs of pups with hyperoxic lung injury, which was augmented upon hUC-MSC administration (Figure 3E and F).

hUC-MSCs treatment modulates hyperoxia-induced lung inflammation and oxidative stress

Total protein levels in BALF were measured as an indication of endothelial and epithelial permeability. Hyperoxia-exposed animals demonstrated elevated BALF protein concentrations compared to normoxia-exposed pups. hUC-MSCs administration (iT or iP) ameliorated the hyperoxia-induced high permeability of the lung epithelium (Figure 4A). The same trend was reflected in MPO expression, an indicator of the number of neutrophils in the lung (Figure 4B).

To further investigate the inflammatory response after hyperoxia exposure, we measured the expression of the pro-inflammatory cytokines TNF- α , IL-1 β , and IL-6 and the anti-inflammatory cytokine IL-10 in the lung tissues using ELISA. The increased TNF- α , IL-1 β , and IL-6 expressions observed in the hyperoxia group were significantly attenuated in both the iT-MSC and iP-MSC groups (Figure 4C-E). Although there was no significant difference in IL-10 expression between the hyperoxic and normoxic groups, we observed an increase in IL-10 expression in rats that received hUC-MSCs iT compared with rats reared in hyperoxia (Figure 4F).

Furthermore, RT-qPCR results confirmed that hyperoxia exposure led to a significant increase in the mRNA expression of the pro-inflammatory mediators macrophage inflammatory protein (*MIP*)-1 α , and *MIP*-1 β . After infusion of hUC-MSCs, iT or iP, the expression of *MIP*-1 α and *MIP*-1 β also significantly decreased (Figure 4G and H). iP administration of hUC-MSCs was slightly more effective in reducing *MIP*-1 α levels than iT administration.

MDA levels in tissues were measured to reflect the oxidative stress. Elevated MDA levels induced by hyperoxia exposure were significantly diminished upon hUC-MSC administration in hyperoxia-exposed rats (Figure 4I).

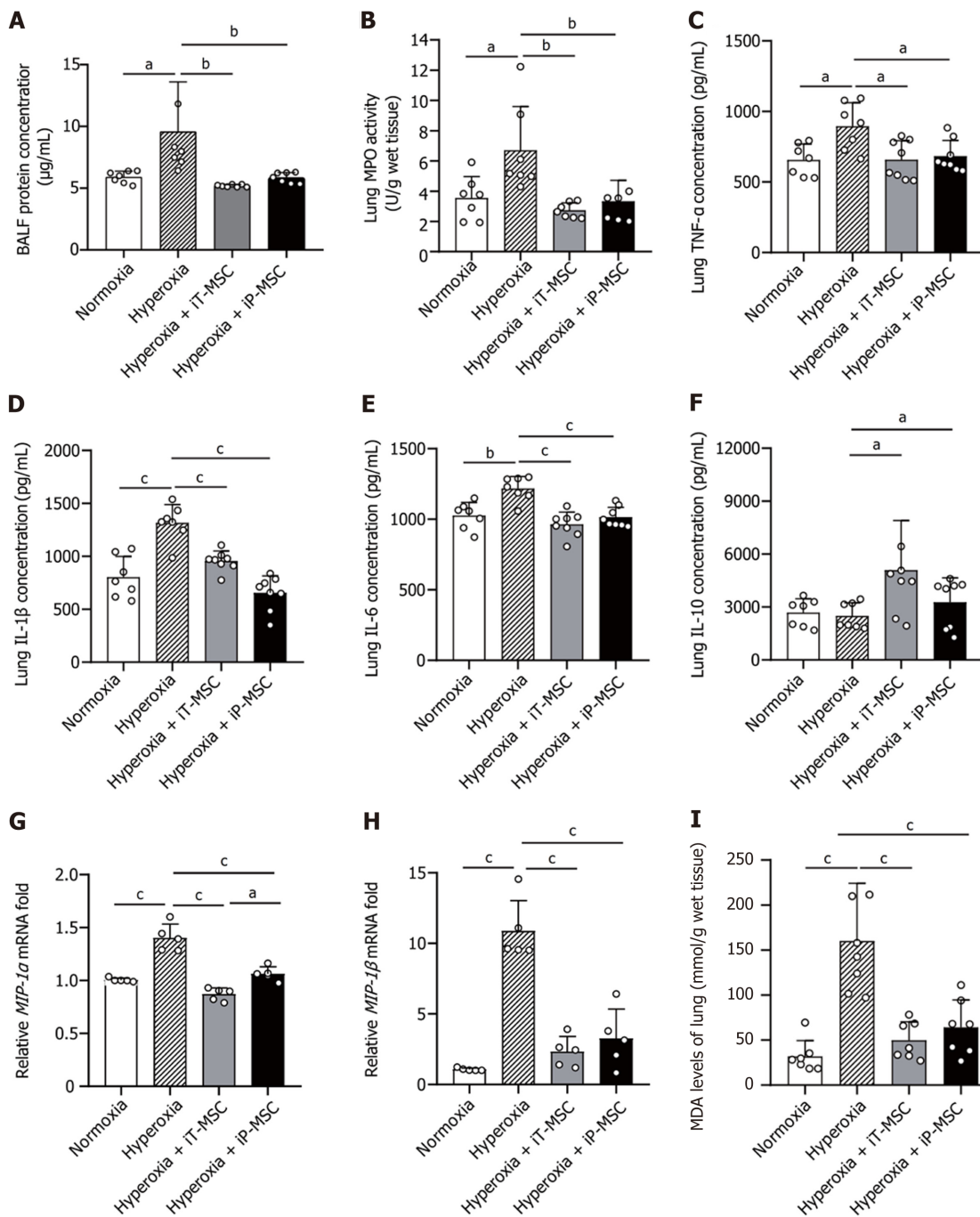
hUC-MSCs treatment modulates the lung transcriptome

We performed a comparative transcriptomic analysis of lung samples from the normoxia, hyperoxia, and hyperoxia + iT-MSC groups *via* RNA-sequencing (Xiuyue Biol, Shandong, China). Hyperoxia-exposed animals showed 1486 significantly enriched and 1720 suppressed mRNAs compared to their normoxic counterparts, while meeting the threshold of an absolute log₂ fold change of ≥ 1 and an adjusted $P < 0.05$. Among the DEGs induced upon hyperoxia exposure, the expression of 880 suppressed genes was increased and that of 1314 upregulated genes was reduced upon hUC-MSCs administration, resulting in a shift in gene expression pattern toward normoxia. The top 100 DEGs are presented in a heat map (Figure 5A). GO analysis indicated that hUC-MSCs treatment blunted these hyperoxia-induced dysregulated genes involved in epithelial cell proliferation (*ENG*, *GPC3*, *ALDH1A2*, *SULF1*), regulation of vasculature development (*CYBB*, *PTPRC*, *CYR61*, *CDH5*, *ANXA3*, *NOTCH4*), positive regulation of cell adhesion (*ALOX15*, *CCDC80*, *CXCL12*), wound healing (*PLET1*, *POSTN*, *MACF1*, *DSP*), and leukocyte migration (*CCL6*, *ITGAL*, *CXCL3*, *LPL*, *CCL9*, *CHST4*), which are biological processes that likely contribute to BPD pathogenesis (Figure 5B). Additionally, five of the most significantly enriched cellular components were extracellular matrix, apical part of the cell, external side of the plasma membrane, receptor complex, and membrane microdomain (Figure 5C). The top five significantly enriched molecular functions were phospholipid binding, signaling receptor activator activity, cell adhesion molecule binding, actin binding, and sulfur compound binding (Figure 5D). Therefore, preliminary RNA-sequencing showed that hyperoxia exposure and hUC-MSCs transplantation caused significant changes in the gene expression, which might serve as novel targets for the treatment of hyperoxia-induced organ injury.

Beneficial effects of hUC-MSCs administration in heart and kidneys in hyperoxia exposed neonatal rats

To quantify the degree of PH-induced RVH, HE stained heart tissue sections were assessed (Figure 6). Exposure to hyperoxia increased the RV free wall thickness and IVS thickness (Figure 6A). The Fulton's index (RV/LV + IVS) showed an increase with hyperoxia exposure (Figure 6D). Both iT and iP administration of hUC-MSCs significantly ameliorated this increase.

Nephrogenesis was assessed on HE stained kidney sections. We observed that, compared to the normoxia group, hyperoxia exposure led to a significant reduction in nephrogenic zone width ($237.9 \pm 35.5 \mu\text{m}$ *vs* $145.3 \pm 23.6 \mu\text{m}$) and glomerular diameter ($70.5 \pm 5.33 \mu\text{m}$ *vs* $43.0 \pm 8.5 \mu\text{m}$). These morphological abnormalities in the heart and kidney were alleviated upon hUC-MSCs administration. In the hyperoxia + iT-MSC group, the averaged nephrogenic zone width and glomerular diameter were $196.7 \pm 25.1 \mu\text{m}$ and $62.1 \pm 5.2 \mu\text{m}$, respectively. In hyperoxia-exposed rats receiving hUC-MSCs iP, the averaged nephrogenic zone width and glomerular diameter were $176.7 \pm 27.8 \mu\text{m}$ and $61.9 \pm 3.5 \mu\text{m}$, respectively (Figure 6B, C, E, and F).



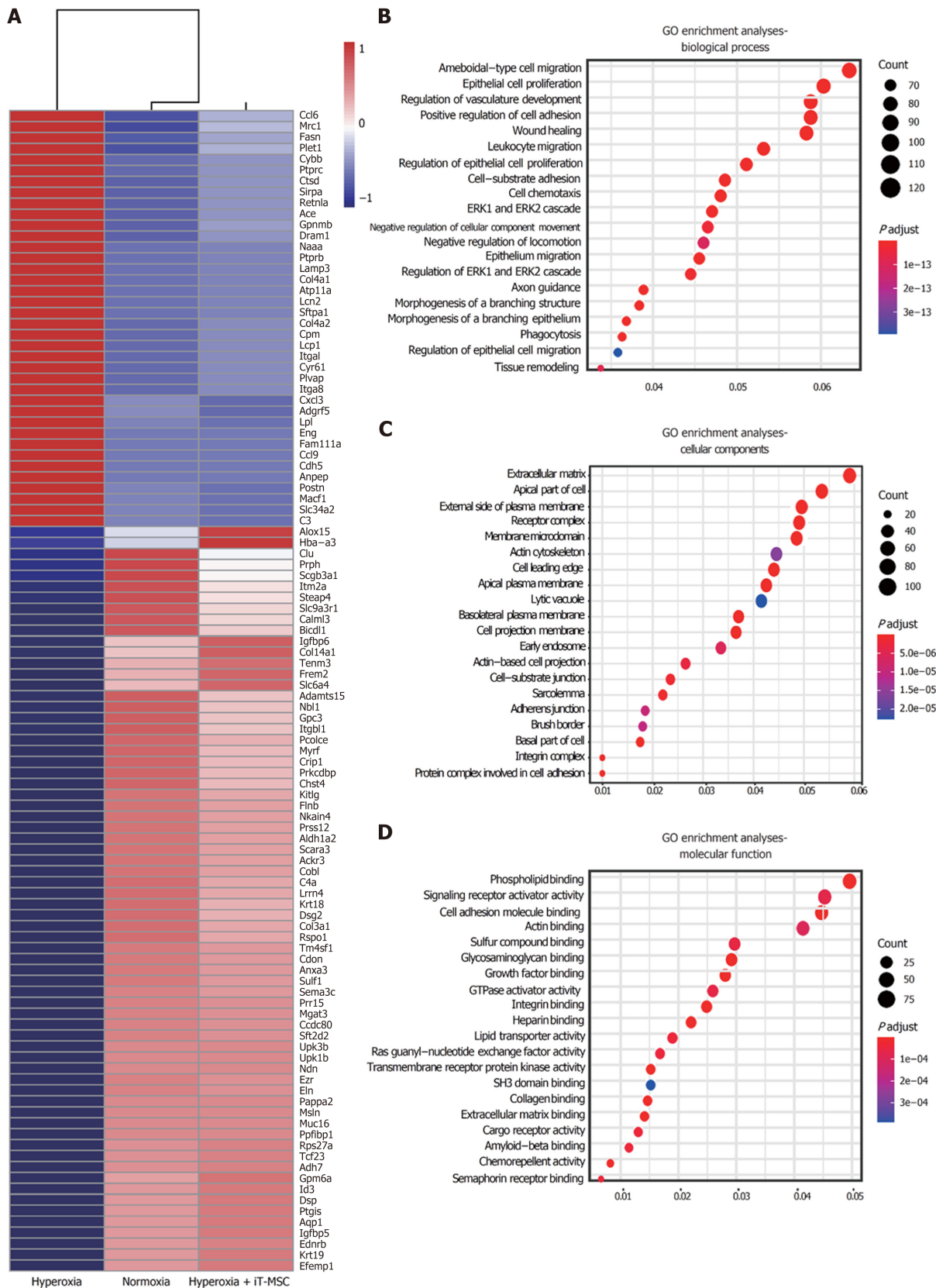
DOI: 10.4252/wjsc.v14.i7.556 Copyright ©The Author(s) 2022.

Figure 4 Human umbilical cord-derived mesenchymal stem cells treatment modulates the hyperoxia-induced lung inflammation and oxidative stress. A: Statistical analyses of overall protein concentration in bronchoalveolar lavage fluid in the four groups ($n = 7$); B-F: Statistical analyses of myeloperoxidase, tumor necrosis factor- α , interleukin (IL)-1 β , IL-6, and IL-10 levels in the lung tissues in the indicated groups ($n = 7$); G and H: Macrophage inflammatory protein (MIP)-1 α and MIP-1 β mRNA expression in the indicated groups ($n = 5$); I: Malondialdehyde levels were measured to evaluate the degree of oxidative reaction in the lung tissues ($n = 7$). ^a $P < 0.05$; ^b $P < 0.01$; ^c $P < 0.001$. iT: Intratracheal; iP: Intraperitoneal; BALF: Bronchoalveolar lavage fluid; MPO: Myeloperoxidase; TNF- α : Tumor necrosis factor- α ; IL: Interleukin; MIP: Macrophage inflammatory protein; MDA: Malondialdehyde; MSC: Mesenchymal stem cell.

Similarly, as *per* the degree of inflammatory and oxidative reactions, MPO expression and MDA levels in the hyperoxia group were elevated compared with those in normoxia in both heart and kidney tissues. Treatment with hUC-MSCs significantly diminished the hyperoxia-induced increase in MPO expression and MDA levels (Figure 6G-J). These parameters did not show a significant statistical difference between iT and iP hUC-MSC administration.

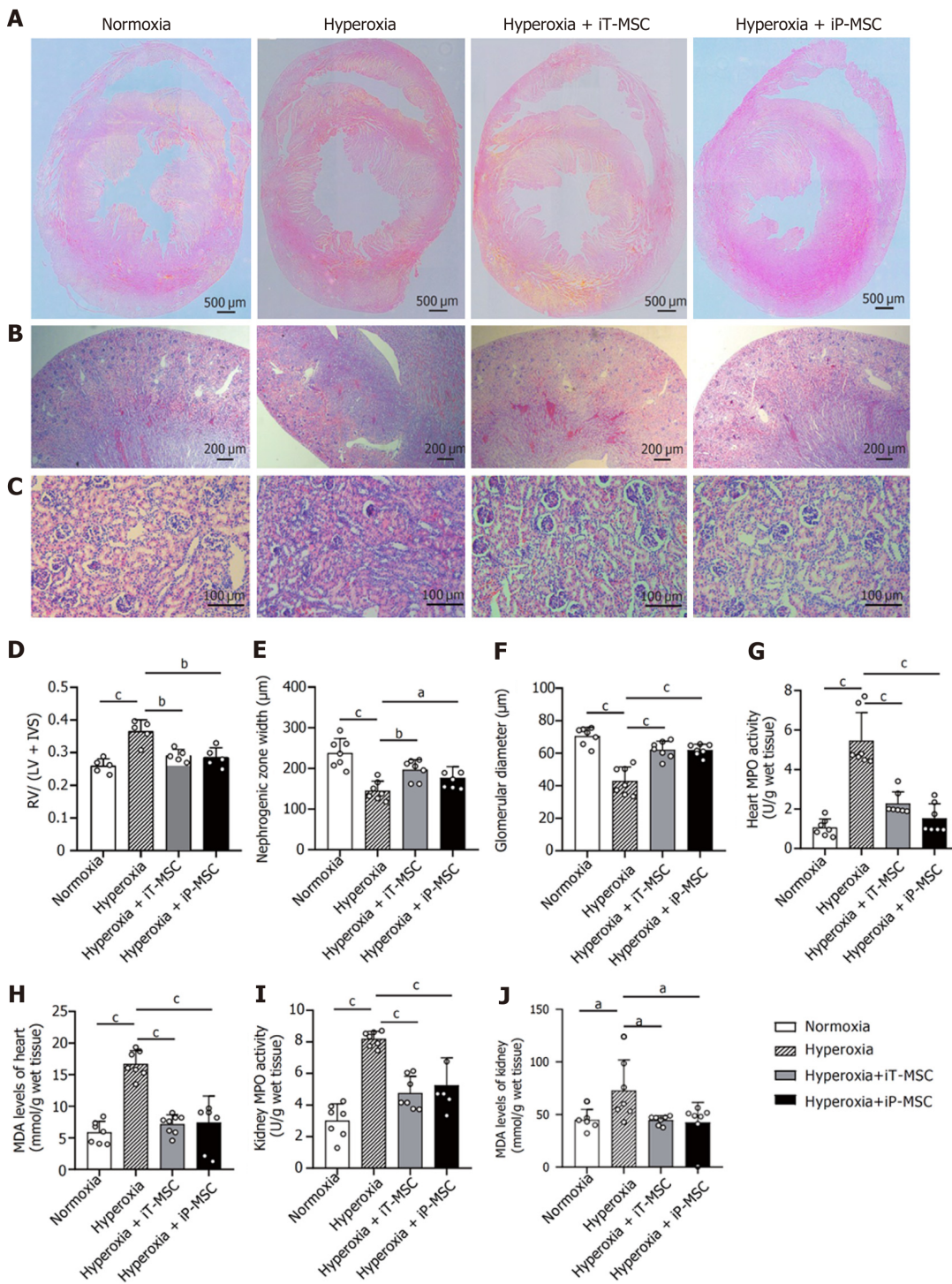
hUC-MSCs activate HO-1 expression and the JAK2/STAT3 signaling pathway to protect against hyperoxia-induced multiple organ injury

To further investigate the mechanism by which hUC-MSCs administration alleviated hyperoxia-induced



DOI: 10.4252/wjsc.v14.i7.556 Copyright ©The Author(s) 2022.

Figure 5 Human umbilical cord-derived mesenchymal stem cells treatment modulates the lung transcriptome. A: The heatmap shows the top 100 differentially expressed genes in lung tissues from the normoxia, hyperoxia, and hyperoxia + intratracheal-mesenchymal stem cell groups. The expression levels of up- and downregulated genes are shown in red and blue, respectively; B-D: Gene ontology analyses of the most significantly affected pathways related to biological process, cellular components, and molecular function. iT: Intratracheal; MSC: Mesenchymal stem cell; GO: Gene ontology.



DOI: 10.4252/wjsc.v14.i7.556 Copyright ©The Author(s) 2022.

Figure 6 Beneficial effects of human umbilical cord-derived mesenchymal stem cells administration in the heart and kidneys of hyperoxic neonatal rats. A: Representative images of harvested heart sections stained with HE for morphometric analyses (scale bars = 500 μm); B and C: Representative photomicrographs of the hematoxylin and eosin stained sections of kidneys obtained at 40 × magnification (scale bars = 200 μm) and 200 × magnification (scale bars = 100 μm) respectively; D: Fulton's index (right ventricle/left ventricle + interventricular septum) was measured to quantify the degree right ventricular hypertrophy (n = 5); E and F: Nephrogenesis was assessed through measuring the width of the nephrogenic zone and the glomerular diameter (n = 7); G–J: Myeloperoxidase and malondialdehyde levels were measured to evaluate the degree of inflammatory and oxidative reaction in heart and kidney tissues respectively (n = 7). *P < 0.05; ^aP < 0.01; ^cP < 0.001. iT: Intratracheal; iP: Intraperitoneal; RV: Right ventricle; LV: Left ventricle; IVS: Interventricular septum; MPO: Myeloperoxidase; MDA: Malondialdehyde; MSC: Mesenchymal stem cell.

lung, heart, and kidney injury in BPD rats, we measured the expression of HO-1 and JAK2/STAT3 signaling pathways in the whole rat lungs, heart, and kidneys. Through gray value quantification, the results of western blotting showed that the expressions of phosphorylated JAK2 (pJAK2), JAK2, phosphorylated STAT3 (pSTAT3), and STAT3 in lungs, heart, and kidneys were significantly suppressed in the hyperoxia group. The expression of the above proteins increased significantly after

hUC-MSCs administration (Figure 7A-E). Hyperoxia exposure significantly increased the expression of HO-1, which was further enhanced in the hUC-MSCs treated groups (Figure 7A and F). These findings imply that the HO-1 and JAK2/STAT3 signaling pathways are associated with the benefits of hUC-MSC therapy in hyperoxic neonatal rats.

DISCUSSION

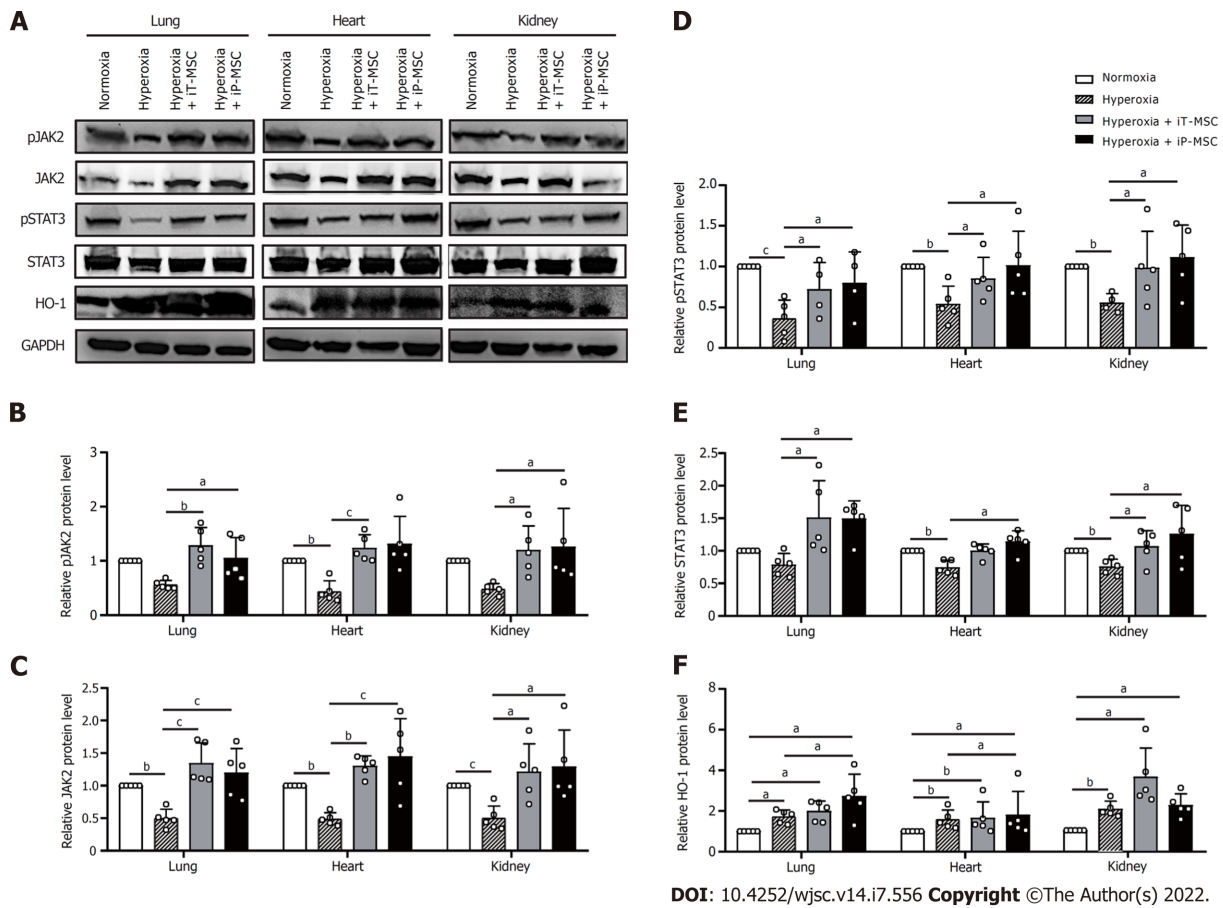
BPD is now recognized as a systemic disease associated with respiratory morbidity, cardiac dysfunction, and neural and renal development impairments[3,12,40,41]. Despite advances in the understanding of BPD pathogenesis, not all the mechanisms that lead to hyperoxia damage are completely understood. The use of allogeneic MSCs, derived from the umbilical cord[16,18], adipose tissue[42], or bone marrow [43], has been recognized as the most promising treatment for BPD. Many experiments and clinical trials have reported that MSC administration, iT[16,18], iP[44], intranasally[45], or intravenously[46], exerts beneficial outcomes with improved lung development, reduced inflammation, and decreased oxidative damage. Moreover, recent studies have demonstrated that MSC-derived exosomes (EXOs) or conditioned medium (CM) containing cytokines, growth factors, and nucleic acids play a critical role in mediating the therapeutic effects of MSCs[17,21]. Notably, we previously showed that iT drip of living human amnion-derived MSCs (hAD-MSCs) is more effective in treating hyperoxia-induced lung injury than hAD-MSC-EXOs or hAD-MSC-CM[42]. This phenomenon can be explained by the fact that living cells survive in the lungs for several days and secrete more exosomes.

Although the protective effects of MSCs or their exosomes on hyperoxia-induced lung injury have been explored by many researchers, the underlying mechanism has not been well studied, and few studies have focused on the therapeutic benefits of systemic multiple organ injury. Hence, based on the above findings, the protective effects of the local administration of hUC-MSCs on systemic multiple organ damage and its underlying mechanisms were investigated in the current study.

The most frequently used animal models of BPD are term-born mice or rats that are exposed to supplemental oxygen, to study the effects of hyperoxia exposure on preterm infants with respiratory distress[1,47]. In this study, we established an experimental newborn rat model *via* prolonged exposure to hyperoxia to induce lung, heart, and kidney injury. The present study showed that the administration of hUC-MSCs on P7 played an essential role in improving pulmonary alveolarization and modulating pulmonary angiogenesis in hyperoxia-exposed rats, although the survival rate did not significantly improve. Specifically, iT hUC-MSCs administration diminished the hyperoxia-induced increase in MLI and vascular smooth muscle thickness and augmented the hyperoxia-induced decrease in peripheral pulmonary vascular density in neonatal rats. We also determined the expression levels of VEGF and PDGF in rats. VEGF is a potent mitogen in endothelial cells that regulates angiogenesis and alveolar development[48]. PDGF is crucial for the alveolarization of normally developing lungs[49]. Our results suggested that treatment with hUC-MSCs augmented the hyperoxia-induced decrease in VEGF and PDGF expression in rats. Thus, we demonstrated that treatment with hUC-MSCs enhanced vascular and alveolar development in neonatal rats through the induction of growth factors.

Inflammation activated during oxidative stress is a common pathway leading to the BPD phenotype [1]. Increased pro-inflammatory cytokine levels found in tracheal aspirates and blood samples from premature infants correlate with an increased risk of BPD[50,51]. Recent studies have suggested that hyperoxia induces pro-inflammatory cytokines and cell infiltration in the alveolar spaces in neonatal Sprague Dawley rats[52]. MDA is the main product of lipid peroxidation and is recognized as a biological marker of oxygen stress injury[53,54]. In this study, rats reared in hyperoxia exhibited a significant increase in BALF protein content, as well as TNF- α , IL-1 β , IL-6, MIP-1 α , MIP-1 β , MPO, and MDA levels, which decreased with hUC-MSC treatment. Additionally, we observed an increase in anti-inflammatory cytokine IL-10 expression in rats that received hUC-MSCs. These results support previous ones[16,55] and suggest that the therapeutic effects of surfactant and hUC-MSCs on hyperoxia-induced lung injury are mediated through the inhibition of pro-inflammatory cytokine production and oxidative stress reactions, as well as the induction of immunosuppressive soluble cytokines such as IL-10.

Subsequently, we performed a comparative transcriptomic analysis of differential gene expression in the lung tissues of rats in the normoxia, hyperoxia, and hyperoxia + iT-MSCs groups. It has been reported that hyperoxia dysregulates the expression of genes that modulate immune response[21,56], oxidative stress[57], cell migration, proliferation, and abnormal airway and pulmonary vascular contractility[58] in an experimental model of hyperoxia-induced BPD. Consistent with previous studies, our findings showed the DEGs in lung tissues induced upon hyperoxia exposure were enriched in pathways related to inflammatory responses, epithelial cell proliferation, and vasculature development. These dysregulated genes could contribute to the observed aberrant pulmonary alveolarization and angiogenesis, increased leukocyte infiltration, and enhanced pro-inflammatory cytokine production. Additionally, we found that hUC-MSCs infusion rescued the abnormally expressed genes, which possibly explains their therapeutic ability in hyperoxia-induced lung injury. Taken together, our findings may provide new evidence for the underlying mechanisms of BPD and MSCs treatment.



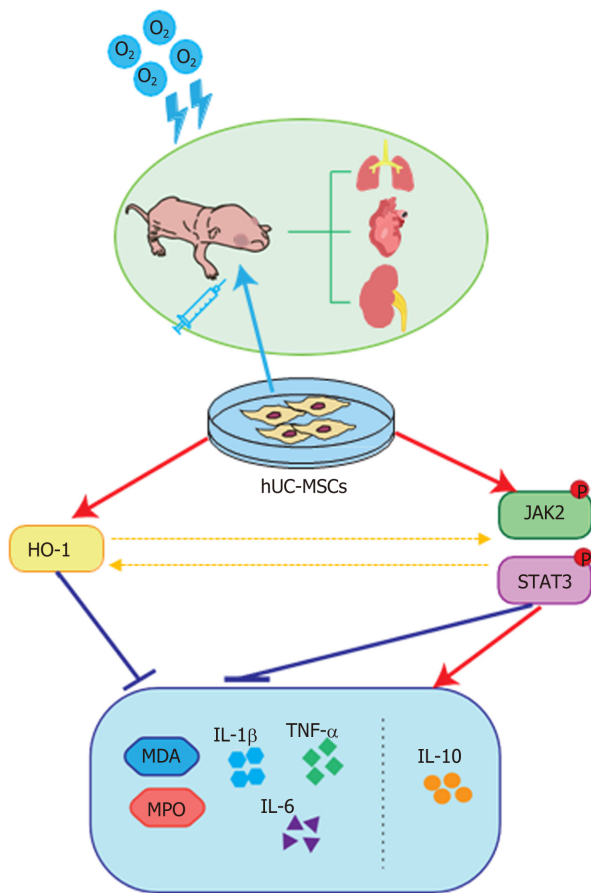
DOI: 10.4252/wjsc.v14.i7.556 Copyright ©The Author(s) 2022.

Figure 7 Human umbilical cord-derived mesenchymal stem cells activated the heme oxygenase-1 and JAK2/STAT3 signaling pathway to protect against hyperoxia-induced multiple-organ injury. A: The protein extracted from tissue homogenates of the lungs, heart, and kidneys were collected for western blotting to detect heme oxygenase-1, JAK2, STAT3 protein expression levels, as well as their phosphorylation; B–F: Statistical analyses of protein expression levels of the above-mentioned genes. ^aP < 0.05; ^bP < 0.01; ^cP < 0.001. iT: Intratracheal; iP: Intraperitoneal; HO-1: Heme oxygenase-1; GAPDH: Glyceraldehyde-3-phosphate dehydrogenase; MSC: Mesenchymal stem cell.

As mentioned above, supraphysiological oxygen concentrations were found to lead to hyperoxia-related PH, ventricular hypertrophy, and renal development impairments, which have been recognized as strong contributors to poor outcomes in preterm infants with BPD[3,4,41]. Of concern, little is known about the treatment outcomes of MSCs in the heart and kidney injuries associated with hyperoxia. In our study, positive results with relieved RVH and nephrogenesis impairment, as well as reduced MPO and MDA levels in the heart and kidney tissues were obtained after iT or iP administration of hUC-MSCs in hyperoxic rat models. Consistent with previous reports, our results suggest additional therapeutic effects of hUC-MSCs administration on histological alterations and modulation of inflammatory cell infiltration and oxidative stress in extrapulmonary organs.

We conducted further experiments to investigate the mechanisms contributing to the therapeutic effects of hUC-MSCs in hyperoxia-exposed animals. The JAK/STAT3 pathway is one of the major pathways involved in many crucial biological processes and is closely associated with many immune and inflammatory diseases[31,59]. Recent studies have indicated that changes in the expression of JAK2 and STAT3 or their phosphorylated forms are related to IL-10 secretion[38,59,60]. Increased IL-10 secretion induced by MSCs in our study has been described previously. Increasing evidence suggests that the JAK2/STAT3 signaling pathway plays a key role in protection against pulmonary[32], cardiac [33,61], and renal injury[34]. The protective effects were inhibited by the selective inhibitors or JAK2/STAT3 siRNA. These studies provided powerful evidence indicating that the activated JAK2/STAT3 signaling pathway is involved in the protective phenotypic changes in injured organs. In line with previous studies, our results showed that JAK2 and STAT3 expression, as well as their phosphorylation, in the lungs, heart, and kidneys were suppressed to some extent in the hyperoxia group and significantly increased after hUC-MSCs treatment.

Among the special defense enzymes developed in mammalian cells to combat oxidative stress, HO-1, an essential enzyme in heme catabolism, has been postulated to play a key role in catalyzing the detoxification of oxidized proteins and modulating the cellular redox homeostasis[26]. In addition, increasing evidence suggests that the products released by the HO reaction possess anti-inflammatory, anti-apoptotic, and anti-proliferative properties[27,62,63]. In the present study, we observed increased HO-1



DOI: 10.4252/wjsc.v14.i7.556 Copyright ©The Author(s) 2022.

Figure 8 Proposed mechanism of therapeutic effects of human umbilical cord-derived mesenchymal stem cells in hyperoxia-induced multiple organ injury. The administration of human umbilical cord-derived mesenchymal stem cells at postnatal day ameliorates hyperoxia-induced lung, heart, and kidney development, and reduces inflammatory and oxidative responses by activating heme oxygenase-1 expression and the JAK/STAT3 pathway. O₂: Oxygen; hUC-MSCs: Human umbilical cord-derived mesenchymal stem cells; HO-1: Heme oxygenase-1; MPO: Myeloperoxidase; TNF- α : Tumor necrosis factor-alpha; IL: Interleukin; MDA: Malondialdehyde.

expression in the hyperoxia-exposed group, which is probably a spontaneous response induced by oxidative stress. Furthermore, our findings suggest that the infusion of hUC-MSCs into neonatal rats further enhanced HO-1 expression. No statistically significant difference in the expressions of these proteins was observed between iT and iP hUC-MSC administration. It has been reported that HO-1 contributes to attenuating hyperoxia-induced pulmonary inflammation, arterial remodeling, and RVH, which were significantly reversed in HO-1 knockout mice or upon tin protoporphyrin IX administration, a HO-1 inhibitor[29,30,64]. Detsika *et al*[65] establish HO-1 as a key regulator to attenuate glomerular injury by using HO-1 deficient rats or rats with HO-1 overexpression targeted to glomerular epithelial cells. Based on these studies, it is considered that elevated HO-1 expression also plays a crucial role in the protective effects of UC-MSCs in alleviating oxidative and inflammatory damage in the lung, heart, and kidney tissues. Moreover, recent studies have demonstrated that HO-1 expression is partly regulated by the JAK/STAT pathway[35]; in turn, the JAK/STAT pathway can be activated by enhanced HO-1 expression[36]. Taken together, we speculate that hUC-MSCs can sense inflammatory and oxidative stimulation and then trigger HO-1 expression, IL-10 secretion, and the JAK2/STAT3 signaling pathway, eventually reducing multiple abnormalities induced by hyperoxia (Figure 8).

Remarkably, the benefits of iT-hUC-MSC administration were equivalent to those of the iP-hUC-MSC administration group. Based on previous studies[66,67] and our investigation, we hypothesized that the beneficial effects of local iT administration of MSCs on hyperoxia-induced systemic multi-organ damage are ascribed to paracrine effects. Considering that the majority of low-birth-weight infants were endotracheal intubated at birth, our study supported that iT-MSC administration is a more convenient and effective administration method.

We acknowledge that there are several limitations to this study. Firstly, we only performed transcriptome sequencing of the whole-lung tissue, which consisted of several types of cells. Gene expression changes of sorted cell subtypes from multiple organs exposed to hyperoxia should be studied and validated in future research to assess the effect of MSCs on different target cell populations and address the underlying molecular mechanisms. Moreover, we observed that hUC-MSCs increased

HO-1 expression and activated the JAK2/STAT3 pathway in the lung, heart, and kidney tissues. However, we merely speculated that these changes in protein expression are involved in the therapeutic changes in the phenotype based on previous studies. Further in-depth mechanistic studies will be needed to validate and understand the molecular mechanisms modulated by hUC-MSCs.

CONCLUSION

In summary, the main findings of our study were that administration of hUC-MSCs significantly ameliorates not only lung injuries but also associated heart and kidney damage in hyperoxia-exposed infant rats. Remarkably, the therapeutic benefits of local iT instillation are equivalent to those of iP administration in hyperoxia-induced systemic multi-organ damage. Additionally, we also demonstrated that the underlying mechanism of the therapeutic effects is presumably the increase in HO-1 expression, IL-10 secretion, and the JAK2/STAT3 signaling pathway. Above all, it is desirable that the present study yield positive results to transform healthcare outcomes for a growing population of premature survivors.

ARTICLE HIGHLIGHTS

Research background

Increasing evidence has suggested that bronchopulmonary dysplasia (BPD) is not merely a lung disease, but a systemic condition with short-term and long-term multiple organ implications. Exposure to hyperoxia causes oxidative stress and contributes to the pathogenesis of these recognized implications, including respiratory morbidity, cardiac dysfunction, and impairments in renal development. Mesenchymal stem cells (MSCs) are multipotent stromal cells that have immunomodulatory, anti-inflammatory, and low immunogenicity properties and have shown great potential for the management of a range of different neonatal conditions, including BPD.

Research motivation

Although the protective effects of MSCs or their exosomes on hyperoxia-induced lung injury have been explored by many researchers, the underlying mechanism has not been addressed in detail, and few studies have focused on their therapeutic benefits on systemic multiple organ injury.

Research objectives

This study aimed to investigate whether intratracheal (iT) administration of human umbilical cord-derived MSCs (hUC-MSCs) could simultaneously attenuate hyperoxia-induced lung, heart, and kidney injuries in an experimental neonatal rat model, and elucidate the underlying regulatory mechanism.

Research methods

We established an experimental newborn rat model *via* prolonged exposure to hyperoxia to induce lung, heart, and kidney injury. Briefly, neonatal rats were exposed to hyperoxia (80% O₂), treated with hUC-MSCs iT or intraperitoneal (iP) on postnatal day 7 (P7), and harvested on postnatal day 21. The tissue sections of the lung, heart, and kidney were analyzed morphometrically. Protein contents of bronchoalveolar lavage fluid (BALF), pulmonary inflammatory cytokines, myeloperoxidase (MPO) expression, and malondialdehyde (MDA) levels were examined. Furthermore, RNA-sequencing, reverse transcription-quantitative polymerase chain reaction and western blot analysis were performed to explore underlying mechanisms.

Research results

The present study showed that the administration of hUC-MSCs on P7 played an essential role in improving pulmonary alveolarization and modulating pulmonary angiogenesis, as well as relieving right ventricular hypertrophy and nephrogenesis impairment in hyperoxia-exposed rats. Rats reared in hyperoxia exhibited a significant increase in BALF protein content, tumor necrosis factor- α , interleukin (IL)-1 β , IL-6, and macrophage inflammatory protein (MIP)-1 α , MIP-1 β , MPO and MDA levels, which decreased with hUC-MSC treatment. Additionally, we observed an increase in anti-inflammatory cytokine IL-10 expression in rats that received hUC-MSCs. Transcriptomic analysis showed that hUC-MSCs administration blunted the hyperoxia-induced dysregulated genes, which were enriched in pathways related to inflammatory responses, epithelial cell proliferation, and vasculature development. Moreover, hUC-MSCs increased heme oxygenase (HO-1), JAK2, and STAT3 expression, and their phosphorylation in the lung, heart, and kidney. Remarkably, no significant difference was observed between iT and iP administration.

Research conclusions

Our results suggest additional therapeutic effects of hUC-MSCs administration on histological alterations, along with the modulation of inflammatory cell infiltration and oxidative stress in extrapulmonary organs. The therapeutic benefits of local iT instillation are equivalent to those of iP administration in systemic multi-organ damage. These therapeutic effects presumably result from an increase in HO-1 expression and the JAK2/STAT3 signaling pathway.

Research perspectives

In future studies, gene expression changes of sorted cell subtypes from multiple organs injured upon hyperoxia exposure will be studied. Further in-depth mechanistic studies are warranted to validate and understand the molecular mechanisms modulated by hUC-MSCs. Moreover, given the significance of changing the MSCs culture mode, the application of genetically modified and three-dimensionally cultured MSCs will be explored to improve therapeutic outcomes in future studies. These studies will lay the foundation for a more extensive and effective clinical application of MSCs in the treatment of BPD.

ACKNOWLEDGEMENTS

The authors sincerely thank Professors Xiu-Li Ju and Dong Li for their guidance in experimental design and discussion.

FOOTNOTES

Author contributions: Dong N and Zhou PP completed the experiment and analyzed the results statistically; Ju XL and Li D proposed the design and conception of the experiment; Zhu HS and Liu LH assisted with the collection of tissue and blood samples from animals and gene expression experiments; Ma HX and Shi Q supervised the animal protocols and integrated the materials; Dong N wrote the first manuscript of the study; Ju XL and Li D revised the manuscript critically; all authors have read and approved the final manuscript.

Supported by Rongxiang Regenerative Medicine Foundation of Shandong University, No. 2019SDRX-18; Clinical Practical New Technology Development Found of Qilu Hospital of Shandong University, No. KYC 2019-0057; Clinical Research Center of Shandong University, No. 2020SDUCRCA010; and Natural Science Foundation of Shandong Province, No. ZR2020MH063.

Institutional review board statement: The study was reviewed and approved by the Ethics Committee on Scientific Research of Qilu Hospital of Shandong University, No. KYLL-2019(KS)-086.

Institutional animal care and use committee statement: All animal procedures and protocols complied with the National Institutes of Health Guide for the Care and Use of Laboratory Animals and were approved by the Ethics Committee on Animal Experiments of Shandong University Qilu Hospital, Jinan, China, No. DWLL-2021-035.

Informed consent statement: All study participants or their legal guardian provided informed written consent about personal and medical data collection prior to study enrolment.

Conflict-of-interest statement: All the authors report no relevant conflicts of interest for this article.

Data sharing statement: No additional data are available.

ARRIVE guidelines statement: The authors have read the ARRIVE guidelines, and the manuscript was prepared and revised according to the ARRIVE guidelines.

Open-Access: This article is an open-access article that was selected by an in-house editor and fully peer-reviewed by external reviewers. It is distributed in accordance with the Creative Commons Attribution NonCommercial (CC BY-NC 4.0) license, which permits others to distribute, remix, adapt, build upon this work non-commercially, and license their derivative works on different terms, provided the original work is properly cited and the use is non-commercial. See: <https://creativecommons.org/licenses/by-nc/4.0/>

Country/Territory of origin: China

ORCID number: Na Dong 0000-0002-0129-5934; Pan-Pan Zhou 0000-0002-1019-6436; Dong Li 0000-0002-6496-4605; Hua-Su Zhu 0000-0001-6432-4555; Ling-Hong Liu 0000-0003-2637-0408; Hui-Xian Ma 0000-0002-8147-8166; Qing Shi 0000-0002-0921-3358; Xiu-Li Ju 0000-0001-5464-3106.

S-Editor: Fan JR

L-Editor: A

P-Editor: Fan JR

REFERENCES

- 1 **Morty RE.** Recent advances in the pathogenesis of BPD. *Semin Perinatol* 2018; **42**: 404-412 [PMID: 30384986 DOI: 10.1053/j.semperi.2018.09.001]
- 2 **Gilfillan M, Bhandari A, Bhandari V.** Diagnosis and management of bronchopulmonary dysplasia. *BMJ* 2021; **375**: n1974 [PMID: 34670756 DOI: 10.1136/bmj.n1974]
- 3 **Thébaud B, Goss KN, Laughon M, Whitsett JA, Abman SH, Steinhorn RH, Aschner JL, Davis PG, McGrath-Morrow SA, Soll RF, Jobe AH.** Bronchopulmonary dysplasia. *Nat Rev Dis Primers* 2019; **5**: 78 [PMID: 31727986 DOI: 10.1038/s41572-019-0127-7]
- 4 **Principi N, Di Pietro GM, Esposito S.** Bronchopulmonary dysplasia: clinical aspects and preventive and therapeutic strategies. *J Transl Med* 2018; **16**: 36 [PMID: 29463286 DOI: 10.1186/s12967-018-1417-7]
- 5 **Davidson LM, Berkelhamer SK.** Bronchopulmonary Dysplasia: Chronic Lung Disease of Infancy and Long-Term Pulmonary Outcomes. *J Clin Med* 2017; **6** [PMID: 28067830 DOI: 10.3390/jcm6010004]
- 6 **Katz TA, Vliegthart RJS, Aarnoudse-Moens CSH, Leemhuis AG, Beuger S, Blok GJ, van Brakel MJM, van den Heuvel MEN, van Kempen AAMW, Lutterman C, Rijpert M, Schiering IA, Ran NC, Visser F, Wilms J, van Kaam AH, Onland W.** Severity of Bronchopulmonary Dysplasia and Neurodevelopmental Outcome at 2 and 5 Years Corrected Age. *J Pediatr* 2022; **243**: 40-46.e2 [PMID: 34929243 DOI: 10.1016/j.jpeds.2021.12.018]
- 7 **Hartnett ME, Penn JS.** Mechanisms and management of retinopathy of prematurity. *N Engl J Med* 2012; **367**: 2515-2526 [PMID: 23268666 DOI: 10.1056/NEJMr1208129]
- 8 **Madan A, Penn JS.** Animal models of oxygen-induced retinopathy. *Front Biosci* 2003; **8**: d1030-d1043 [PMID: 12700061 DOI: 10.2741/1056]
- 9 **White SL, Perkovic V, Cass A, Chang CL, Poulter NR, Spector T, Haysom L, Craig JC, Salmi IA, Chadban SJ, Huxley RR.** Is low birth weight an antecedent of CKD in later life? *Am J Kidney Dis* 2009; **54**: 248-261 [PMID: 19339091 DOI: 10.1053/j.ajkd.2008.12.042]
- 10 **Chow JC, Chou HC, Hwang J, Chen CM.** Anti-Tn Monoclonal Antibody Ameliorates Hyperoxia-Induced Kidney Injury by Suppressing Oxidative Stress and Inflammation in Neonatal Mice. *Mediators Inflamm* 2021; **2021**: 1180543 [PMID: 34720748 DOI: 10.1155/2021/1180543]
- 11 **Smit B, Smulders YM, van der Wouden JC, Oudemans-van Straaten HM, Spoelstra-de Man AME.** Hemodynamic effects of acute hyperoxia: systematic review and meta-analysis. *Crit Care* 2018; **22**: 45 [PMID: 29477145 DOI: 10.1186/s13054-018-1968-2]
- 12 **de Visser YP, Walther FJ, Laghmani el H, Steendijk P, Middeldorp M, van der Laarse A, Wagenaar GT.** Phosphodiesterase 4 inhibition attenuates persistent heart and lung injury by neonatal hyperoxia in rats. *Am J Physiol Lung Cell Mol Physiol* 2012; **302**: L56-L67 [PMID: 21949154 DOI: 10.1152/ajplung.00041.2011]
- 13 **Ramani M, Bradley WE, Dell'Italia LJ, Ambalavanan N.** Early exposure to hyperoxia or hypoxia adversely impacts cardiopulmonary development. *Am J Respir Cell Mol Biol* 2015; **52**: 594-602 [PMID: 25255042 DOI: 10.1165/rcmb.2013-0491OC]
- 14 **Menon RT, Shrestha AK, Reynolds CL, Barrios R, Shivanna B.** Long-term pulmonary and cardiovascular morbidities of neonatal hyperoxia exposure in mice. *Int J Biochem Cell Biol* 2018; **94**: 119-124 [PMID: 29223466 DOI: 10.1016/j.biocel.2017.12.001]
- 15 **Mohr J, Voggel J, Vohlen C, Dinger K, Dafinger C, Fink G, Göbel H, Liebau MC, Dötsch J, Alejandro Alcazar MA.** IL-6/Smad2 signaling mediates acute kidney injury and regeneration in a murine model of neonatal hyperoxia. *FASEB J* 2019; **33**: 5887-5902 [PMID: 30721632 DOI: 10.1096/fj.201801875RR]
- 16 **Chou HC, Chang CH, Chen CH, Lin W, Chen CM.** Consecutive daily administration of intratracheal surfactant and human umbilical cord-derived mesenchymal stem cells attenuates hyperoxia-induced lung injury in neonatal rats. *Stem Cell Res Ther* 2021; **12**: 258 [PMID: 33933128 DOI: 10.1186/s13287-021-02335-4]
- 17 **Porzionato A, Zaramella P, Dedja A, Guidolin D, Van Wemmel K, Macchi V, Jurga M, Perilongo G, De Caro R, Baraldi E, Muraca M.** Intratracheal administration of clinical-grade mesenchymal stem cell-derived extracellular vesicles reduces lung injury in a rat model of bronchopulmonary dysplasia. *Am J Physiol Lung Cell Mol Physiol* 2019; **316**: L6-L19 [PMID: 30284924 DOI: 10.1152/ajplung.00109.2018]
- 18 **Chang YS, Choi SJ, Sung DK, Kim SY, Oh W, Yang YS, Park WS.** Intratracheal transplantation of human umbilical cord blood-derived mesenchymal stem cells dose-dependently attenuates hyperoxia-induced lung injury in neonatal rats. *Cell Transplant* 2011; **20**: 1843-1854 [PMID: 23167961 DOI: 10.3727/096368911X565038]
- 19 **Pierro M, Ionescu L, Montemurro T, Vadivel A, Weissmann G, Oudit G, Emery D, Bodiga S, Eaton F, Péault B, Mosca F, Lazzari L, Thébaud B.** Short-term, long-term and paracrine effect of human umbilical cord-derived stem cells in lung injury prevention and repair in experimental bronchopulmonary dysplasia. *Thorax* 2013; **68**: 475-484 [PMID: 23212278 DOI: 10.1136/thoraxjnl-2012-202323]
- 20 **Pierro M, Thébaud B, Soll R.** Mesenchymal stem cells for the prevention and treatment of bronchopulmonary dysplasia in preterm infants. *Cochrane Database Syst Rev* 2017; **11**: CD011932 [PMID: 29125893 DOI: 10.1002/14651858.CD011932.pub2]
- 21 **Willis GR, Fernandez-Gonzalez A, Anastas J, Vitali SH, Liu X, Ericsson M, Kwong A, Mitsialis SA, Kourembanas S.** Mesenchymal Stromal Cell Exosomes Ameliorate Experimental Bronchopulmonary Dysplasia and Restore Lung Function through Macrophage Immunomodulation. *Am J Respir Crit Care Med* 2018; **197**: 104-116 [PMID: 28853608 DOI: 10.1164/rccm.201705-0925OC]

- 22 **Liang X**, Ding Y, Zhang Y, Tse HF, Lian Q. Paracrine mechanisms of mesenchymal stem cell-based therapy: current status and perspectives. *Cell Transplant* 2014; **23**: 1045-1059 [PMID: [23676629](#) DOI: [10.3727/096368913X667709](#)]
- 23 **Kern S**, Eichler H, Stoeve J, Klüter H, Bieback K. Comparative analysis of mesenchymal stem cells from bone marrow, umbilical cord blood, or adipose tissue. *Stem Cells* 2006; **24**: 1294-1301 [PMID: [16410387](#) DOI: [10.1634/stemcells.2005-0342](#)]
- 24 **Lin KC**, Yeh JN, Chen YL, Chiang JY, Sung PH, Lee FY, Guo J, Yip HK. Xenogeneic and Allogeneic Mesenchymal Stem Cells Effectively Protect the Lung Against Ischemia-reperfusion Injury Through Downregulating the Inflammatory, Oxidative Stress, and Autophagic Signaling Pathways in Rat. *Cell Transplant* 2020; **29**: 963689720954140 [PMID: [33050736](#) DOI: [10.1177/0963689720954140](#)]
- 25 **Gutiérrez-Fernández M**, Rodríguez-Frutos B, Ramos-Cejudo J, Otero-Ortega L, Fuentes B, Vallejo-Cremades MT, Sanz-Cuesta BE, Díez-Tejedor E. Comparison between xenogeneic and allogeneic adipose mesenchymal stem cells in the treatment of acute cerebral infarct: proof of concept in rats. *J Transl Med* 2015; **13**: 46 [PMID: [25637958](#) DOI: [10.1186/s12967-015-0406-3](#)]
- 26 **Gozzelino R**, Jeney V, Soares MP. Mechanisms of cell protection by heme oxygenase-1. *Annu Rev Pharmacol Toxicol* 2010; **50**: 323-354 [PMID: [20055707](#) DOI: [10.1146/annurev.pharmtox.010909.105600](#)]
- 27 **Ryter SW**, Choi AM. Targeting heme oxygenase-1 and carbon monoxide for therapeutic modulation of inflammation. *Transl Res* 2016; **167**: 7-34 [PMID: [26166253](#) DOI: [10.1016/j.trsl.2015.06.011](#)]
- 28 **Luo YY**, Wu SH, Lu HY, Li BJ, Li SJ, Sun ZY, Jin R, Chen XQ. Lipoxin A4 attenuates hyperoxia-induced lung epithelial cell injury via the upregulation of heme oxygenase1 and inhibition of proinflammatory cytokines. *Mol Med Rep* 2020; **21**: 429-437 [PMID: [31746387](#) DOI: [10.3892/mmr.2019.10821](#)]
- 29 **Dunigan-Russell K**, Silverberg M, Lin VY, Li R, Wall SB, Li Q, Nicola T, Gotham J, Crowe DR, Vitiello PF, Agarwal A, Tipple TE. Club Cell Heme Oxygenase-1 Deletion: Effects in Hyperoxia-Exposed Adult Mice. *Oxid Med Cell Longev* 2020; **2020**: 2908271 [PMID: [32587658](#) DOI: [10.1155/2020/2908271](#)]
- 30 **Fernandez-Gonzalez A**, Alex Mitsialis S, Liu X, Kourembanas S. Vasculoprotective effects of heme oxygenase-1 in a murine model of hyperoxia-induced bronchopulmonary dysplasia. *Am J Physiol Lung Cell Mol Physiol* 2012; **302**: L775-L784 [PMID: [22287607](#) DOI: [10.1152/ajplung.00196.2011](#)]
- 31 **Owen KL**, Brockwell NK, Parker BS. JAK-STAT Signaling: A Double-Edged Sword of Immune Regulation and Cancer Progression. *Cancers (Basel)* 2019; **11** [PMID: [31842362](#) DOI: [10.3390/cancers11122002](#)]
- 32 **Liu W**, Gao Y, Li H, Wang H, Ye M, Jiang G, Chen Y, Liu Y, Kong J, Liu W, Sun M, Hou M, Yu K. Intravenous transplantation of mesenchymal stromal cells has therapeutic effects in a sepsis mouse model through inhibition of septic natural killer cells. *Int J Biochem Cell Biol* 2016; **79**: 93-103 [PMID: [27521657](#) DOI: [10.1016/j.biocel.2016.08.013](#)]
- 33 **Zhang L**, Wang X, Zhang H, Feng M, Ding J, Zhang B, Cheng Z, Qian L. Exercise-induced peptide EIP-22 protect myocardial from ischaemia/reperfusion injury via activating JAK2/STAT3 signalling pathway. *J Cell Mol Med* 2021; **25**: 3560-3572 [PMID: [33710777](#) DOI: [10.1111/jcmm.16441](#)]
- 34 **Liu Y**, Wang L, Du Y, Chen Z, Guo J, Weng X, Wang X, Wang M, Chen D, Liu X. Effects of apigenin pretreatment against renal ischemia/reperfusion injury via activation of the JAK2/STAT3 pathway. *Biomed Pharmacother* 2017; **95**: 1799-1808 [PMID: [28962085](#) DOI: [10.1016/j.biopha.2017.09.091](#)]
- 35 **Tron K**, Samoylenko A, Musikowski G, Kobe F, Immenschuh S, Schaper F, Ramadori G, Kietzmann T. Regulation of rat heme oxygenase-1 expression by interleukin-6 via the Jak/STAT pathway in hepatocytes. *J Hepatol* 2006; **45**: 72-80 [PMID: [16510205](#) DOI: [10.1016/j.jhep.2005.12.019](#)]
- 36 **Yan X**, Cheng X, He X, Zheng W, Yuan X, Chen H. HO-1 Overexpressed Mesenchymal Stem Cells Ameliorate Sepsis-Associated Acute Kidney Injury by Activating JAK/stat3 Pathway. *Cell Mol Bioeng* 2018; **11**: 509-518 [PMID: [31719896](#) DOI: [10.1007/s12195-018-0540-0](#)]
- 37 **Lee PJ**, Camhi SL, Chin BY, Alam J, Choi AM. AP-1 and STAT mediate hyperoxia-induced gene transcription of heme oxygenase-1. *Am J Physiol Lung Cell Mol Physiol* 2000; **279**: L175-L182 [PMID: [10893216](#) DOI: [10.1152/ajplung.2000.279.1.L175](#)]
- 38 **Zhu HS**, Li D, Li C, Huang JX, Chen SS, Li LB, Shi Q, Ju XL. Prior transfusion of umbilical cord mesenchymal stem cells can effectively alleviate symptoms of motion sickness in mice through interleukin 10 secretion. *World J Stem Cells* 2021; **13**: 177-192 [PMID: [33708346](#) DOI: [10.4252/wjSC.v13.i2.177](#)]
- 39 **Chen CM**, Chou HC, Lin W, Tseng C. Surfactant effects on the viability and function of human mesenchymal stem cells: *in vitro* and *in vivo* assessment. *Stem Cell Res Ther* 2017; **8**: 180 [PMID: [28774314](#) DOI: [10.1186/s13287-017-0634-y](#)]
- 40 **Reich B**, Hoeber D, Bendix I, Felderhoff-Mueser U. Hyperoxia and the Immature Brain. *Dev Neurosci* 2016; **38**: 311-330 [PMID: [28152539](#) DOI: [10.1159/000454917](#)]
- 41 **Xu X**, You K, Bu R. Proximal Tubular Development Is Impaired with Downregulation of MAPK/ERK Signaling, HIF-1 α , and Catalase by Hyperoxia Exposure in Neonatal Rats. *Oxid Med Cell Longev* 2019; **2019**: 9219847 [PMID: [31558952](#) DOI: [10.1155/2019/9219847](#)]
- 42 **Li Z**, Gong X, Li D, Yang X, Shi Q, Ju X. Intratracheal Transplantation of Amnion-Derived Mesenchymal Stem Cells Ameliorates Hyperoxia-Induced Neonatal Hyperoxic Lung Injury via Aminoacyl-Peptide Hydrolase. *Int J Stem Cells* 2020; **13**: 221-236 [PMID: [32323511](#) DOI: [10.15283/ijsc.191110](#)]
- 43 **Xie Y**, Chen F, Jia L, Chen R, Zhang VW, Zhong X, Wang D. Mesenchymal stem cells from different sources show distinct therapeutic effects in hyperoxia-induced bronchopulmonary dysplasia in rats. *J Cell Mol Med* 2021; **25**: 8558-8566 [PMID: [34322990](#) DOI: [10.1111/jcmm.16817](#)]
- 44 **Chang YS**, Oh W, Choi SJ, Sung DK, Kim SY, Choi EY, Kang S, Jin HJ, Yang YS, Park WS. Human umbilical cord blood-derived mesenchymal stem cells attenuate hyperoxia-induced lung injury in neonatal rats. *Cell Transplant* 2009; **18**: 869-886 [PMID: [19500472](#) DOI: [10.3727/096368909X471189](#)]
- 45 **Moreira A**, Winter C, Joy J, Winter L, Jones M, Noronha M, Porter M, Quim K, Corral A, Alayli Y, Seno T, Mustafa S, Hornsby P, Ahuja S. Intranasal delivery of human umbilical cord Wharton's jelly mesenchymal stromal cells restores lung alveolarization and vascularization in experimental bronchopulmonary dysplasia. *Stem Cells Transl Med* 2020; **9**: 221-234 [PMID: [31774626](#) DOI: [10.1002/sctm.18-0273](#)]

- 46 **Álvarez-Fuente M**, Arruzza L, Lopez-Ortego P, Moreno L, Ramírez-Orellana M, Labrandero C, González Á, Melen G, Cerro MJD. Off-label mesenchymal stromal cell treatment in two infants with severe bronchopulmonary dysplasia: clinical course and biomarkers profile. *Cytotherapy* 2018; **20**: 1337-1344 [PMID: 30327248 DOI: 10.1016/j.jcyt.2018.09.003]
- 47 **O'Reilly M**, Thébaud B. Animal models of bronchopulmonary dysplasia. The term rat models. *Am J Physiol Lung Cell Mol Physiol* 2014; **307**: L948-L958 [PMID: 25305248 DOI: 10.1152/ajplung.00160.2014]
- 48 **Yun EJ**, Lorizio W, Seedorf G, Abman SH, Vu TH. VEGF and endothelium-derived retinoic acid regulate lung vascular and alveolar development. *Am J Physiol Lung Cell Mol Physiol* 2016; **310**: L287-L298 [PMID: 26566904 DOI: 10.1152/ajplung.00229.2015]
- 49 **Lindahl P**, Boström H, Karlsson L, Hellström M, Kalén M, Betsholtz C. Role of platelet-derived growth factors in angiogenesis and alveogenesis. *Curr Top Pathol* 1999; **93**: 27-33 [PMID: 10339896 DOI: 10.1007/978-3-642-58456-5_4]
- 50 **Tullus K**, Noack GW, Burman LG, Nilsson R, Wretling B, Brauner A. Elevated cytokine levels in tracheobronchial aspirate fluids from ventilator treated neonates with bronchopulmonary dysplasia. *Eur J Pediatr* 1996; **155**: 112-116 [PMID: 8775225 DOI: 10.1007/BF02075762]
- 51 **D'Angio CT**, Ambalavanan N, Carlo WA, McDonald SA, Skogstrand K, Hougaard DM, Shankaran S, Goldberg RN, Ehrenkranz RA, Tyson JE, Stoll BJ, Das A, Higgins RD; Eunice Kennedy Shriver National Institute of Child Health and Human Development Neonatal Research Network. Blood Cytokine Profiles Associated with Distinct Patterns of Bronchopulmonary Dysplasia among Extremely Low Birth Weight Infants. *J Pediatr* 2016; **174**: 45-51.e5 [PMID: 27117196 DOI: 10.1016/j.jpeds.2016.03.058]
- 52 **Wang Y**, Yue S, Luo Z, Cao C, Yu X, Liao Z, Wang M. N-methyl-D-aspartate receptor activation mediates lung fibroblast proliferation and differentiation in hyperoxia-induced chronic lung disease in newborn rats. *Respir Res* 2016; **17**: 136 [PMID: 27769245 DOI: 10.1186/s12931-016-0453-1]
- 53 **Zhang J**, Yang Z, Zhang S, Xie Z, Han S, Wang L, Zhang B, Sun S. Investigation of endogenous malondialdehyde through fluorescent probe MDA-6 during oxidative stress. *Anal Chim Acta* 2020; **1116**: 9-15 [PMID: 32389192 DOI: 10.1016/j.aca.2020.04.030]
- 54 **Del Rio D**, Stewart AJ, Pellegrini N. A review of recent studies on malondialdehyde as toxic molecule and biological marker of oxidative stress. *Nutr Metab Cardiovasc Dis* 2005; **15**: 316-328 [PMID: 16054557 DOI: 10.1016/j.numecd.2005.05.003]
- 55 **Chen CM**, Chou HC. Human mesenchymal stem cells attenuate hyperoxia-induced lung injury through inhibition of the renin-angiotensin system in newborn rats. *Am J Transl Res* 2018; **10**: 2628-2635 [PMID: 30210699]
- 56 **Revhaug C**, Bik-Multanowski M, Zasada M, Rognlien AGW, Günther CC, Książek T, Madetko-Talowska A, Szewczyk K, Grabowska A, Kwinta P, Pietrzyk JJ, Baumbusch LO, Saugstad OD. Immune System Regulation Affected by a Murine Experimental Model of Bronchopulmonary Dysplasia: Genomic and Epigenetic Findings. *Neonatology* 2019; **116**: 269-277 [PMID: 31454811 DOI: 10.1159/000501461]
- 57 **Bhattacharya S**, Zhou Z, Yee M, Chu CY, Lopez AM, Lunger VA, Solleti SK, Resseguie E, Buczynski B, Mariani TJ, O'Reilly MA. The genome-wide transcriptional response to neonatal hyperoxia identifies Ahr as a key regulator. *Am J Physiol Lung Cell Mol Physiol* 2014; **307**: L516-L523 [PMID: 25150061 DOI: 10.1152/ajplung.00200.2014]
- 58 **Shrestha AK**, Gopal VYN, Menon RT, Hagan JL, Huang S, Shivanna B. Lung omics signatures in a bronchopulmonary dysplasia and pulmonary hypertension-like murine model. *Am J Physiol Lung Cell Mol Physiol* 2018; **315**: L734-L741 [PMID: 30047283 DOI: 10.1152/ajplung.00183.2018]
- 59 **Murray PJ**. The JAK-STAT signaling pathway: input and output integration. *J Immunol* 2007; **178**: 2623-2629 [PMID: 17312100 DOI: 10.4049/jimmunol.178.5.2623]
- 60 **Li L**, Zhang J, Chen J, Xu-Monette ZY, Miao Y, Xiao M, Young KH, Wang S, Medeiros LJ, Wang M, Ford RJ, Pham LV. B-cell receptor-mediated NFATc1 activation induces IL-10/STAT3/PD-L1 signaling in diffuse large B-cell lymphoma. *Blood* 2018; **132**: 1805-1817 [PMID: 30209121 DOI: 10.1182/blood-2018-03-841015]
- 61 **Qiao S**, Mao X, Wang Y, Lei S, Liu Y, Wang T, Wong GT, Cheung CW, Xia Z, Irwin MG. Remifentanyl Preconditioning Reduces Postischemic Myocardial Infarction and Improves Left Ventricular Performance via Activation of the Janus Activated Kinase-2/Signal Transducers and Activators of Transcription-3 Signal Pathway and Subsequent Inhibition of Glycogen Synthase Kinase-3 β in Rats. *Crit Care Med* 2016; **44**: e131-e145 [PMID: 26468894 DOI: 10.1097/CCM.0000000000001350]
- 62 **Otterbein LE**, Soares MP, Yamashita K, Bach FH. Heme oxygenase-1: unleashing the protective properties of heme. *Trends Immunol* 2003; **24**: 449-455 [PMID: 12909459 DOI: 10.1016/s1471-4906(03)00181-9]
- 63 **Brouard S**, Otterbein LE, Anrather J, Tobiasch E, Bach FH, Choi AM, Soares MP. Carbon monoxide generated by heme oxygenase 1 suppresses endothelial cell apoptosis. *J Exp Med* 2000; **192**: 1015-1026 [PMID: 11015442 DOI: 10.1084/jem.192.7.1015]
- 64 **Suliman HB**, Keenan JE, Piantadosi CA. Mitochondrial quality-control dysregulation in conditional HO-1^{-/-} mice. *JCI Insight* 2017; **2**: e89676 [PMID: 28194437 DOI: 10.1172/jci.insight.89676]
- 65 **Detsika MG**, Duann P, Atsaves V, Papalouis A, Lianos EA. Heme Oxygenase 1 Up-Regulates Glomerular Decay Accelerating Factor Expression and Minimizes Complement Deposition and Injury. *Am J Pathol* 2016; **186**: 2833-2845 [PMID: 27662796 DOI: 10.1016/j.ajpath.2016.07.009]
- 66 **Lee JW**, Fang X, Krasnodembskaya A, Howard JP, Matthay MA. Concise review: Mesenchymal stem cells for acute lung injury: role of paracrine soluble factors. *Stem Cells* 2011; **29**: 913-919 [PMID: 21506195 DOI: 10.1002/stem.643]
- 67 **Liang OD**, Mitsialis SA, Chang MS, Vergadi E, Lee C, Aslam M, Fernandez-Gonzalez A, Liu X, Baveja R, Kourembanas S. Mesenchymal stromal cells expressing heme oxygenase-1 reverse pulmonary hypertension. *Stem Cells* 2011; **29**: 99-107 [PMID: 20957739 DOI: 10.1002/stem.548]



Published by **Baishideng Publishing Group Inc**
7041 Koll Center Parkway, Suite 160, Pleasanton, CA 94566, USA
Telephone: +1-925-3991568
E-mail: bpgoffice@wjgnet.com
Help Desk: <https://www.f6publishing.com/helpdesk>
<https://www.wjgnet.com>

